Therapeutic Targeting of TGF Ligands in Glioblastoma Using Novel Antisense Oligonucleotides Reduces the Growth of Experimental Gliomas

Papachristodoulou, Alexandros ; Silginer, Manuela ; Weller, Michael ; Schneider, Hannah ; Hasenbach, Kathy ; Janicot, Michel ; Roth, Patrick

Abstract: PURPOSE Transforming growth factor (TGF)- is expressed at high levels by glioma cells and contributes to the malignant phenotype of glioblastoma. However, its therapeutic targeting remains challenging. Here, we examined an alternative therapeutic approach of TGF inhibition using two novel phosphorothioate-locked nucleic acid (LNA)-modified antisense oligonucleotide gapmers, ISTH1047 and ISTH0047, which specifically target TGF and TGF . EXPERIMENTAL DESIGN We characterized the effects of ISTH1047 and ISTH0047 on TGF expression, downstream signaling and growth of human LN-308, LN-229, and ZH-161 cells as well as murine SMA-560 glioma cells . Furthermore, we assessed their target inhibition and effects on survival in orthotopic xenogeneic and syngeneic rodent glioma models . RESULTS Both antisense oligonucleotides specifically silenced their corresponding target and abrogated SMAD2 phosphorylation in several glioma cell lines. Moreover, inhibition of TGF or TGF expression by ISTH1047 or ISTH0047 reduced the migration and invasiveness of LN-308 and SMA-560 glioma cells. Systemic antisense oligonucleotide administration to glioma-bearing mice suppressed or mRNA expression as well as the expression of the downstream target in orthotopic gliomas. Glioma-bearing mice had significantly prolonged survival upon systemic treatment with ISTH1047 or ISTH0047, which was associated with a reduction of intratumoral SMAD2 phosphorylation and, in a fully immunocompetent model, with increased immune cell infiltration. CONCLUSIONS Targeting TGF expression with the novel LNA antisense oligonucleotides ISTH1047 or ISTH0047 results in strong antiglioma activity and , which may represent a promising approach to be examined in human patients with glioma.

DOI: https://doi.org/10.1158/1078-0432.CCR-17-3024

Therapeutic targeting of TGF-β ligands in glioblastoma using novel antisense oligonucleotides reduces the growth of experimental gliomas

Alexandros Papachristodoulou[1*#], Manuela Silginer[1#], Michael Weller[1], Hannah Schneider[1], Kathy Hasenbach[2], Michel Janicot[2], Patrick Roth[1]

[1]Laboratory of Molecular Neuro-Oncology, Department of Neurology, University Hospital Zurich and University of Zurich, Switzerland; [2]Isarna Therapeutics GmbH, Munich, Germany; [*]Present address: Departments of Urology and Pathology and Cell Biology, Herbert Irving Comprehensive Cancer Center, Columbia University, 1139 St. Nicholas Avenue, 10032 New York, USA

[#] These authors contributed equally.

Corresponding author: Patrick Roth, MD, Department of Neurology, University Hospital Zurich and University of Zurich, Frauenklinikstrasse 26, 8091 Zurich, Switzerland, Phone: +41 (0)44 2555511, Fax: +41- (0)44 255 4380, E-mail: patrick.roth@usz.ch

Conflict of interest: PR has received honoraria for advisory boards and lectures from BMS, Roche, MSD, Novartis, Novocure, Covagen, Virometix and Molecular Partners. MW has received research grants from Abbvie, Adastra, Bayer, Isarna, Merck, Sharp & Dohme (MSD), EMD Pharmaceuticals, Piqur and Roche and honoraria for lectures or advisory board participation from Abbvie, Celgene, MSD, EMD Pharmaceuticals, Pfizer, Roche and Teva. KH and MJ are employees of Isarna. AP, MS and HS have nothing to disclose.

Running title: Anti-glioma effect of antisense-mediated TGF-β inhibition

Keywords: Glioblastoma, TGF-β_1, TGF-β_2, antisense oligonucleotide, pSMAD2

Statement of translational relevance

Transforming growth factor (TGF)-β has been attributed an important role in glioblastoma progression and may be a key player in tumor invasion, angiogenesis and immunosuppression. Targeting the TGF-β pathway has been regarded a promising therapeutic strategic but the approaches used to date have failed due to insufficient inhibition of the TGF-β pathway or dose-limiting toxicity. In this study, we directly inhibited TGF-β_1 or TGF-β_2 expression with novel second-generation antisense oligonucleotides (ASO). We demonstrate that ASO-mediated TGF-β inhibition reduces the invasive potential of glioma cells, while increasing the number of tumor-infiltrating immune cells. These novel TGF-β-targeting ASO reach the tumor upon systemic administration and prolong survival of both immunocompetent and immune-deficient mice bearing orthotopic gliomas. Therefore, this study represents a major improvement in TGF-β-targeted therapy, with high promise for clinical translation in human glioma patients.

Abstract

Purpose: Transforming growth factor (TGF)-β is expressed at high levels by glioma cells and contributes to the malignant phenotype of glioblastoma. However, its therapeutic targeting remains challenging. Here, we examined an alternative therapeutic approach of TGF-β inhibition using two novel phosphorothioate-locked nucleic acid (LNA)-modified antisense oligonucleotide gapmers, ISTH1047 and ISTH0047, which specifically target TGF-β_1 and TGF-β_2.

Experimental design: We characterized the effects of ISTH1047 and ISTH0047 on TGF-$\beta_{1/2}$ expression, downstream signaling and growth of human LN-308, LN-229 and ZH-161 cells as well as murine SMA-560 glioma cells *in vitro*. Furthermore, we assessed their target inhibition and effects on survival in orthotopic xenogeneic and syngeneic rodent glioma models *in vivo*.

Results: Both antisense oligonucleotides specifically silenced their corresponding target and abrogated SMAD2 phosphorylation in several glioma cell lines. Moreover, inhibition of TGF-β_1 or TGF-β_2 expression by ISTH1047 or ISTH0047 reduced migration and invasiveness of LN-308 and SMA-560 glioma cells. Systemic ASO administration to glioma-bearing mice suppressed *TGF-β_1* or *TGF-β_2* mRNA expression as well as the expression of the down-stream target *PAI-1* in orthotopic gliomas. Glioma-bearing mice had significantly prolonged survival upon systemic treatment with ISTH1047 or ISTH0047, which was associated with a reduction of intratumoral SMAD2 phosphorylation and, in a fully immunocompetent model, with increased immune cell infiltration.

Conclusions: Targeting TGF-β expression with the novel LNA antisense oligonucleotides ISTH1047 or ISTH0047 results in strong anti-glioma activity *in vitro* and *in vivo* which may represent a promising approach to be examined in human glioma patients.

Introduction

Glioblastoma is the most lethal primary tumor of the central nervous system (CNS) in adults. The current standard of care for newly diagnosed glioblastoma includes surgical resection followed by radiotherapy and chemotherapy with the alkylating agent, temozolomide (TMZ). However, the median survival of glioblastoma patients is still limited to approximately 16 months with a 5-year survival rate of less than 10% within clinical trials (1). A key mediator of the malignant phenotype of glioma cells is transforming growth factor (TGF)-β. It has pleiotropic functions and exists as three different mature ligands, TGF-β_1, TGF-β_2 and TGF-β_3 (2). All are involved in the phosphorylation of SMAD2 and SMAD3 proteins which are responsible for transcriptional regulation of genes involved in tumor infiltration and epithelial to mesenchymal transition (EMT), but also immunosuppression and angiogenesis (3,4). Elevated levels of TGF-β as well as the activation of the TGF-β/SMAD cascade correlates with high tumor grade and in some cases with poor prognosis in glioblastoma patients (5,6). Gliomas generate an immunosuppressive tumor microenvironment through the secretion of a variety of cytokines, including TGF-β that can impede anti-tumor immune responses (3). Furthermore, TGF-β signaling enhances the invasiveness and migratory ability of glioma cells and maintains a drug-resistant stem cell phenotype (7,8). Consequently, targeting the TGF-β pathway represents an attractive therapeutic approach. In this regard, various strategies have been explored *in vitro* and *in vivo* including gene transfer of TGF-β scavengers such as decorin (9), furin protease inhibitors which interfere with the processing of TGF-β (10) or indirect TGF-β signaling targeting through integrin inhibition (11). The most advanced approaches comprise TGF-β receptor (TGF-βR)-1 inhibitors

such as SD-208 (12), galunisertib (13) or LY2109761 (14) and the pan TGF-β antibody, 1D11 (15). Despite promising pre-clinical data, these agents failed to show a clear clinical benefit in glioblastoma patients (16,17). Therefore, the clinical development of most of these drugs has been stopped because of lack of activity, most likely due to insufficient target inhibition or dose-limiting toxicity (16).

Antisense oligonucleotides (ASO) are single-stranded, biochemically-modified deoxyribonucleotide molecules that are 15–25 nucleotides in length. They are designed as complementary sequences to a target gene's mRNA thereby specifically inhibiting gene expression (18). The concept of ASO-mediated gene silencing has emerged as a potentially powerful alternative or concomitant treatment to conventional cancer therapy. There is a plethora of genes related to cancer progression or therapeutic resistance which cannot be targeted efficiently with antibodies or small molecules but possibly with ASO. Because of their targeted mode of action, ASO may be less toxic than many conventional anti-tumor therapeutics (19). One of the most clinically advanced TGF-β-targeting approaches involved the locoregional application of AP12009 (trabedersen), a first generation ASO with a sequence complementary to human TGF-β_2 mRNA, in a randomized phase II trial in patients with recurrent anaplastic glioma or glioblastoma. Even though AP12009 was not inferior to standard chemotherapy, no convincing efficacy signal was seen (20).

Given the insufficient results obtained with the TGF-β-targeting strategies explored so far, we aimed at assessing TGF-β signaling inhibition in glioma models using two novel second-generation phosphorothioate-locked nucleic acid (LNA)-modified ASO. The chemical structure of LNA-modified ASO offers significant advantages such as increased

binding affinity and higher tissue concentrations (21,22). Here, we assessed the anti-glioma activity of two novel LNA-modified ASO molecules which specifically target TGF-β_1 (ISTH1047) or TGF-β_2 (ISTH0047) in several *in vitro* and *in vivo* glioma models.

Materials and methods

Reagents and cell lines

The human malignant glioma cell lines LN-308 and LN-229 were kindly provided by Dr. N. de Tribolet (Lausanne, Switzerland). The mouse glioma cell line SMA-560 was derived from a spontaneous astrocytoma in a VM/Dk mouse (23) and provided by Dr. D. Bigner (Durham, NC). The glioma cell lines were maintained in Dulbecco's modified Eagle's medium supplemented with 10% fetal calf serum (Biochrom, Minneapolis, MN) and 2 mmol/L L-glutamine (Gibco Life Technologies, Paisley, UK). The glioma-initiating cell (GIC) line ZH-161 was established after informed consent and approval of the Swiss ethical committees and characterized in detail (24). ZH-161 cells were grown in Neurobasal medium supplemented with 2 µl/ml B-27 without vitamin A, 2 mM L-glutamine (Gibco Life Technologies), fibroblast growth factor (FGF)-2 and epidermal growth factor (EGF) (20 ng/mL each, Peprotech, Rocky Hill, PA). All cells were grown in a humidified 37ºC incubator with 5% CO_2. ISTH1047, ISTH0047 and C3_ISTH0047 (scrambled control) antisense oligonucleotides were designed and provided by ISARNA Therapeutics GmbH (Munich, Germany). ISTH1047, targeting TGF-β_1 (sequence TCGATGCGCTTCCG), and ISTH0047, targeting TGF-β_2 (sequence CAAAGTATTTGGTCTCC), represent 14-mer and 17-mer, full locked nucleic acid (LNA)-modified antisense oligonucleotide gapmers (Suppl. Fig. 1). The specificity of each ASO was confirmed via the NCBI BLAST® software (https://blast.ncbi.nlm.nih.gov/Blast.cgi) to align oligonucleotides to human and murine TGF-β_1 or TGF-β_2 sequences (Suppl. Fig. 2). Digoxigenin (DIG)-labelled ISTH1047 was also provided by ISARNA Therapeutics GmbH. Recombinant human TGF-$\beta_{1/2}$ was purchased from R&D Systems (Minneapolis,

MN). SD-208 was provided by Scios (Fremont, CA) and galunisertib (LY2157299) by Eli Lilly Co (Indianapolis, IN).

Real-time quantitative PCR

Total RNA was isolated with the NucleoSpin System (Macherey-Nagel, Düren, Germany) and cDNA was retro-transcribed using Invitrogen Superscript II reverse transcriptase (ThermoFisher Scientific, Waltham, MA). For real-time quantitative PCR, cDNA amplification was quantified using SYBR Green chemistry on the 7300 Real time PCR System (Applied Biosystems, Zug, Switzerland). The conditions for the PCR reactions were: 40 cycles, 95 °C/15 sec, 60 °C/1 min. Human and mouse HPRT1 transcript levels were used as a reference for relative quantification of mRNA expression levels via the ΔCT_t method (25). The following specific primers were used: *human HPRT1* fwd: 5'-TGA GGA TTT GGA AAG GGT GT-3'; *human HPRT1* rev: 5'-GAG CAC ACA GAG GGC TAC AA-3'; *human TGF-β_1* fwd: 5'-GCC CTG GAC ACC AAC TAT TG-3'; *human TGF-β_1* rev: 5'-CGT GTC CAG GCT CCA AAT G-3'; *human TGF-β_2* fwd: 5'-AAG CTT ACA CTG TCC CTG CTG C-3'; *human TGF-β_2* rev: 5'-TGT GGA GGT GCC ATC AAT ACC T-3'; *human TGF-β_3* fwd: 5′-ATG ACC CAC GTC CCC TAT CA-3′, *human TGF-β_3* rev: 5′-CAG ACA GCC AGT TCG TTG TG-3′; *mouse HPRT1* fwd: 5'-TTG CTG ACC TGC TGG ATT AC-3'; *mouse HPRT1* rev: 5'-TTT ATG TCC CCC GTT GAC TG-3'; *mouse TGF-β_1* fwd: 5'-CTC CCG TGG CTT CTA GTG C-3'; *mouse TGF-β_1* rev: 5'-GCC TTA GTT TGG ACA GGA TCT G-3'; *mouse TGF-β_2* fwd: 5'-TCG ACA TGG CTT CTA GTG C-3'; *mouse TGF-β_2* rev: 5'-CCC TGG TAC TGT TGT AGA TGG A-3'; *mouse TGF-β_3* fwd: 5′-AGCATCCACTGTCCATGTCA-3′, *mouse TGF-β_3* rev: 5′-TTCTTCCTCTGACTGCCCTG-3′; *mouse plasminogen activator inhibitor (PAI)-1* fwd: 5'-TCT GGG AAA GGG TTC ACT

TTA CC-3', *mouse plasminogen activator inhibitor (PAI)-1* rev: 5'-GAC ACG CCA TAG GGA GAG AAG-3'. For expression analysis of human targets in the oligonucleotide-treated xenograft mouse model, the following human-specific primers, which do not recognize the mouse *TGF-β1,* TGF-*β2* or *TGF-β3* isoforms, were used: *TGF-β1* fwd: 5′-CAATTCCTGGCGATACCTCAG-3′; *TGF-β1* rev: 5′-GCACAACTCCGGTGACATCAA-3′; *TGF-β2* fwd: 5′-CAGCACACTCGATATGGACCA-3′; *TGF-β2* rev: 5′-CCTCGGGCTCAGGATAGTCT-3′; *TGF-β3* fwd: 5′-AACGGTGATGACCCACGTC-3′, *TGF-β3* rev: 5′-CCGACTCGGTGTTTTCCTGG-3′; *PAI1* fwd: 5′-CAGAAAGTGAAGATCGAGGTGAAC-3′; *PAI1* rev: 5′-GGAAGGGTCTGTCCATGATGAA-3′.

Immunoblot

Whole protein lysates were generated by lysing the cells with lysis buffer P (26). Denatured whole protein lysates and concentrated supernatants (30 µg/lane) were separated on 10-15% acrylamide gels. After transfer to nitrocellulose (Biorad, Hercules, CA), blots were blocked in 5% milk-TBST and incubated overnight at 4°C with primary antibodies specific for: total SMAD2 (clone 86F7, Cell Signaling, Boston, MA) phosphorylated SMAD2 (pSMAD2) (clone 138D4, Cell Signaling), total SMAD3 (Cell Signaling), phosphorylated SMAD3 (pSMAD3) (clone C25A9, Cell Signaling), total AKT (Cell Signaling), phosphorylated AKT (pAKT) (Cell Signaling) and β-actin (clone sc-1616, Santa Cruz Biotechnologies, Santa Cruz, CA). The membranes were then washed in TBST and incubated for 1 h at room temperature with horseradish peroxidase (HRP)-coupled secondary antibodies: anti-rabbit or anti-goat (clones sc-2004 and sc-2033,

231 Santa Cruz Biotechnologies). Protein bands were visualized by enhanced
232 chemoluminescence (Pierce/Thermo Fisher, Madison, WI).
233
234 *Animal studies*
235 All procedures were performed in accordance with the Cantonal Veterinary Office Zurich
236 and Federal Food Safety and Veterinary Office. For the xenograft models, Crl: CD1 Foxn1
237 nude mice were purchased from Charles River Laboratories (Wilmington, MA). For the
238 syngeneic studies, VM/Dk mice were bred in house. Mice of 6-10 weeks of age were used
239 in all experiments. Mice were anaesthetized using an intraperitoneal 3 component
240 injection consisting of fentanyl, midazolam and medetomidin (26). For intracranial tumor
241 cell implantation, the mice were fixed under a stereotactic device (Stoelting, Wood Dale,
242 IL) and a burr hole was drilled in the skull 2 mm lateral and 1 mm posterior to the bregma.
243 A Hamilton syringe needle was introduced to a depth of 3 mm. LN-308, LN-229 or ZH-
244 161 human glioma cells (10^5) or SMA-560 murine glioma cells ($5x10^3$) in a volume of 2 µl
245 PBS were injected into the right striatum of Crl: CD1 Foxn1 nude or VM/Dk mice,
246 respectively. C3_ISTH0047 (20 mg/kg), ISTH1047 (10 mg/kg) or ISTH0047 (20 mg/kg)
247 were injected subcutaneously for five consecutive days for studies that aimed at
248 assessing target inhibition. Forty-eight hours after the last injection, all mice were PBS-
249 perfused and organs were harvested for further analyses. For survival studies, C3_ ISTH
250 0047 (20 mg/kg), ISTH1047 (10 mg/kg) or ISTH0047 (20 mg/kg) were injected
251 subcutaneously for five consecutive days and then twice weekly. Mice were monitored
252 daily for neurological symptoms according to Cantonal Veterinary Office Zurich guidelines
253 and euthanized when exhibiting grade 2 symptoms: grade 0 - no visible impairment;

grade 1 - reduced activity, slight imbalance, balance and coordination impairments; grade 2 – decreased to no activity, 15% weight loss compared with peak weight measured on tumor inoculation day, slight paralysis of left legs and moderate signs of pain (26). Treatment was started at day 5 after tumor cell inoculation for VM/Dk mice and at day 25 (LN-308) or day 10 (LN-229, ZH-161) after tumor cell injection for Crl: CD1 Foxn1 nude animals. For the assessment of oligonucleotide delivery to the brain, digoxigenin (DIG)-labelled ISTH1047 (10 mg/kg) was subcutaneously injected for two consecutive days and the mice were PBS-perfused 48 h after the last injection. For liver enzyme analyses, blood was collected from LN-308-bearing mice on the day the first animal became symptomatic and sent for aspartate transaminase (ASAT) and alanine transaminase (ALAT) quantification at the Laboratory for Veterinary Medicine (University of Zurich, Switzerland).

Statistical analysis

Data were derived from experiments performed at least twice in triplicates with similar results. Quantitative data are presented as mean ± standard deviation (SD). Statistical significance was assessed using one-way ANOVA using Bonferroni correction as a post-hoc test. All statistical analyses were performed using Prism 5 (GraphPad Software, La Jolla, CA) at $p<0.05$ or $p<0.01$.

Additional methods are described in the Supplementary data.

Results

ISTH1047 and ISTH0047 decrease TGF-β$_{1/2}$ expression and abrogate TGF-β signaling in glioma cells *in vitro*

Based on the chosen sequence, ISTH1047 and ISTH0047 were designed as antisense oligonucleotides specifically inhibiting TGF-β$_1$ or TGF-β$_2$ (Suppl Fig. 1,2). First, we examined the biological effects of both oligonucleotides in human LN-308 and mouse SMA-560 glioma cells *in vitro*. ISTH1047 down-regulated TGF-β$_1$ protein levels up to 96 h post-transfection in both cell lines, whereas ISTH0047 reduced TGF-β$_2$ protein levels for up to 96 h in LN-308 cells and 72 h in SMA-560 cells (Fig. 1A,B). Increasing concentrations of both oligonucleotides reduced the expression of their corresponding target TGF-β ligand at mRNA level, reaching the highest inhibition efficiency at 50 nM or more in both cell lines (Suppl Fig. 3A,B). Moreover, *TGF-β$_1$* or *TGF-β$_2$* mRNA levels were significantly reduced up to 72 h post-transfection in human LN-308, LN-229 and ZH-161 glioma cells as well as the murine glioma cell line SMA-560. *TGF-β$_3$* mRNA levels were not significantly affected after ASO transfection in LN-308 or SMA-560 cells, but ISTH0047 exposure increased *TGF-β$_3$* levels in LN-229 cells and reduced *TGF-β$_3$* mRNA levels in ZH-161 cells (Fig. 1C). We observed a reduction of intracellular SMAD2 phosphorylation with increasing concentrations of ISTH1047 or ISTH0047 in LN-308 and SMA-560 cells. ISTH1047 diminished pSMAD2 starting at a concentration of 3.13 nM and ISTH0047 at 12.5 nM in LN-308 cells (Suppl Fig. 3C). In SMA-560 cells, ISTH1047 abrogated SMAD2 phosphorylation at 50 nM, while ISTH0047 exerted strongest effects at 100 nM (Suppl Fig. 3D). Total SMAD2 levels were not altered upon ISTH1047 or ISTH0047 transfection in either cell line (Suppl Fig. 3C,D). The decrease of pSMAD2

299 levels occurred at 48 h after transfection (Fig. 1D). Similarly, pSMAD3 levels were
300 reduced in both LN-308 and SMA-560 cells. To assess the effect of *TGF-β_1* or *TGF-β_2*
301 inhibition on alternative *TGF-β* signaling pathways, we examined the phosphorylation
302 levels of AKT 48 h after ASO exposure. pAKT was reduced following exposure to
303 ISTH1047 or ISTH0047 only in LN-308 cells (Fig. 1E). In line with these findings, exposure
304 to ISTH1047 or ISTH0047 reduced pSMAD2 and pSMAD3 expression in LN-229 cells
305 and the GIC line ZH-161. No consistent effect of ASO-mediated *TGF-β* inhibition on
306 pAKT levels was observed in these cells (Fig. 1F).
307
308 **Oligonucleotide-driven TGF-β inhibition impairs glioma cell migration and invasion**
309 We went on to examine the biological effects of ISTH1047 and ISTH0047 on the viability
310 and clonogenicity of glioma cells. A concentration of 50 nM of either oligonucleotide alone
311 had no impact on cell viability (Suppl. Fig. 4A,B). Moreover, in clonogenic survival assays,
312 transfection with either oligonucleotide had no effect in LN-308 cells although ISTH1047
313 reduced colony formation of SMA-560 cells (Suppl. Fig. 4C,D). Migration and invasion
314 into the surrounding tissue can be induced by TGF-β and are among the hallmarks of
315 glioblastoma. Exposure to ISTH1047 reduced migration of LN-308 and SMA-560 cells in
316 Boyden chamber assays. A similar inhibition of glioma cell migration was observed with
317 ISTH0047. Conversely, addition of exogenous TGF-$\beta_{1/2}$ resulted in increased glioma cell
318 migration (Fig. 2A,B; Suppl. Fig. 5). To assess whether the two oligonucleotides impair
319 invasiveness of glioma cells, we performed spheroid invasion assays into a three-
320 dimensional collagen I gel. Spheroid invasion was significantly reduced following TGF-
321 β_1- or -β_2-specific oligonucleotide transfection for up to 96 h in LN-308 cells, while

exogenous TGF-β_1 stimulation increased invasiveness at 96 h (Fig. 2C; Suppl. Fig. 6A). In SMA-560 cells, ISTH1047 transfection blocked spheroid formation in agar. Targeting TGF-β_2 using ISTH0047 led to a significant reduction in spheroid invasion, whereas stimulation with exogenous TGF-β_2 increased the invasion of SMA-560 cells (Fig. 2D; Suppl. Fig. 6B).

TGF$\beta_{1/2}$ inhibition in murine glioma models *in vivo*

Because of the strong anti-TGF-β activity of the two ASO molecules observed *in vitro*, we aimed at exploring target down-regulation *in vivo* using the xenogeneic LN-308 as well as the syngeneic SMA-560 model. To this end, we determined whether systemically administered ISTH1047 or ISTH0047 reach the tumor site and inhibit TGF-β_1 or TGF-β_2 expression in experimental gliomas. DIG-labelled ISTH1047 was detected specifically in the tumor region upon systemic administration in mice bearing LN-308- or SMA-560-derived gliomas (Fig. 3A-E). Moreover, systemic administration of ISTH1047 or ISTH0047 to mice with intracranially growing gliomas resulted in a significant down-regulation of *TGF-β_1* or *TGF-β_2* mRNA expression levels, respectively, in the tumor-bearing hemisphere without significantly altering *TGF-β_3* levels (Fig. 3F). To examine whether the observed target down-regulation had an effect on TGF-β-dependent downstream signaling, we assessed the expression of PAI1, a classical *TGF-β* response gene (27). Indeed, *PAI1* mRNA levels were significantly down-regulated in gliomas derived from LN-308 or SMA-560 cells following systemic treatment with ISTH1047 or ISTH0047 (Fig. 3G). Expression levels of all assessed targets were up-regulated in the tumor-bearing hemisphere compared to the normal counterpart, apart from *TGF-β_2* and *TGF-β_3* levels

345 in the SMA-560 model. *TGF-β_2* levels were also reduced after ISTH0047 treatment in the
346 normal hemisphere in both glioma models (Fig. 3F,G).
347 After confirmation of ASO delivery and target inhibition in experimental gliomas, we
348 assessed effects on survival. Systemic treatment with either ASO prolonged survival of
349 mice with orthotopically growing xenogeneic LN-308- or syngeneic SMA-560-derived
350 gliomas (Fig. 4A,G). Tumor volumes were reduced in mice receiving ISTH1047 or
351 ISTH0047 treatment in both models (Fig. 4B,H). In LN-229-bearing mice, although only
352 ISTH0047 exerted a significant survival benefit, neither treatment reduced the tumor
353 volume at an early time point of analysis (Fig. 4C,D; Suppl. Fig.7). On the contrary, in the
354 ZH-161 model, we observed a significantly reduced tumor burden in mice treated with
355 ISTH0047 that exhibited a non-significant trend for better survival compared to control-
356 treated mice (Fig. 4E,F). Furthermore, treatment with ISTH1047 or ISTH0047 reduced
357 tumoral SMAD2 phosphorylation in LN-308-, LN-229- and SMA-560-bearing mice (Fig.
358 5). The number of invasive glioma satellites was also decreased in gliomas of mice
359 treated with TGF-β-targeting ASO (Suppl. Fig. 8).
360 For a detailed evaluation of host cell infiltration in the tumor, we assessed the frequencies
361 of different immune cell populations after ISTH1047 or ISTH0047 treatment in the
362 syngeneic, immunocompetent SMA-560 glioma model. We observed a significant
363 increase in the $CD45^+$ leukocyte population in ISTH0047-treated mice, which correlated
364 with an increased infiltration by $CD3^+$ T cells (Fig. 6A,B). Although $CD45^+/CD3^+$ cells
365 exhibited an increase by trend only in ISTH1047-treated mice, the cytotoxic $CD8^+$ T cell
366 population was significantly enriched in the tumors of mice treated with either ISTH1047
367 or ISTH0047 (Fig. 6C). $CD4^+$ T cells and $CD11b^+$ macrophage/microglial cells were not

more frequent in the tumor upon ASO treatment (Fig. 6D,E). In terms of blood vessel density, ISTH0047 reduced the number of $CD31^+$ endothelial cells (Suppl. Fig. 9). Finally, treatment with either oligonucleotide alone was well tolerated without significant weight loss. Blood analyses of mice treated with ISTH1047 demonstrated increased aspartate transaminase (ASAT) and alanine transaminase (ALAT) levels, without any clinically apparent adverse symptoms (Suppl. Fig. 10).

Discussion

TGF-β signaling represents a central hub orchestrating various biological functions that are involved in the malignant phenotype of glioblastoma. TGF-β_1 and TGF-β_2 are significantly upregulated compared to normal brain tissue, and the expression of TGF-β_1 correlates with the expression of the target gene *PAI1* (6). Therefore, a ligand-based approach to directly inhibit TGF-β_1 or TGF-β_2 with ASO represents an attractive therapeutic strategy. The promising but inconclusive results of a trial assessing the local administration of a first generation ASO targeting human TGF-β_2 mRNA (20) led to the development of two second generation LNA-modified ASO, ISTH1047 and ISTH0047 targeting TGF-β_1 and TGF-β_2, respectively (Suppl. Fig. 1) that can be administered systemically. ISTH1047 and ISTH0047 are second-generation ASO that benefit from the addition of LNA modifications, which increase their RNA binding affinity and confer enhanced nuclease resistance versus first-generation molecules (28). Here, we characterized the anti-glioma activity of these novel ASO in human and mouse glioma models *in vitro* and *in vivo*.

TGF-β_1 or TGF-β_2 levels were significantly reduced in various human and mouse glioma cells upon exposure to either ASO at low concentrations (Fig. 1A-C; Suppl Fig. 3A,B), indicating that both molecules result in strong target inhibition. In contrast, AP12009 achieved a significant TGF-β_2 reduction only in the µM range (29). Since a biologically meaningful TGF-β inhibition should lead to a reduction of canonical SMAD-dependent signaling, we initially examined this pathway in several glioma cell lines. Both ASO reduced SMAD2 phosphorylation more potently than TGF-βRI kinase inhibition by SD-208 (Fig. 1D), denoting a potential benefit of these novel ASO in targeting TGF-β/SMAD

410 signaling against adenosine tri-phosphate (ATP)-competitive inhibitors *in vitro*. In line with
411 our findings, another approach targeting TGF-β ligands using adenoviral transfer of
412 soluble TGFβRI and II, resulted in an almost complete reduction of pSMAD2 levels in
413 glioma cells (30). Indirect approaches against the TGF-β/SMAD2 signaling axis, e.g., via
414 integrin inhibition have also proven to inhibit glioma progression in preclinical models
415 (11,31). Iintegrin αvβ8 is upregulated in high grade gliomas and plays a crucial role in
416 TGF-β_1 activation and subsequent SMAD2 signaling. αvβ8 inhibition decreased both
417 TGF-$\beta_{1/2}$ bioavailability inducing almost complete SMAD2 dephosphorylation in LN-308
418 and LN-229 glioma cells (11). In the current study we show that blocking either TGF-β_1
419 or TGF-β_2 expression using ASO approaches, results in a similarly strong reduction of
420 pSMAD2 levels, suggesting that direct inhibition of a single isoform is sufficient to
421 abrogate TGF-β/SMAD2 signaling (32,33). Although the exact mechanism for this
422 remains elusive, we conclude that depleting a single TGF-β isoform may impair auto-
423 feedback loops resulting in strong reduction of pSMAD2 levels, despite the presence of
424 other isoforms (26,34,35). While similar suppression was detected at the level of another
425 canonical target, pSMAD3, less activity was seen when exploring pAKT as a
426 representative non-canonical target of TGF-β, yet, non-canonical signaling in response
427 to TGF-β is less prominent in our models (Fig. 1E,F). We have recently revealed an
428 unexpected role for TGF-β_3 in the regulation of downstream TGF-β signaling despite high
429 expression of the other two isoforms in glioblastoma (26). Here, blocking TGF-β_1 or TGF-
430 β_2 expression influenced TGF-β_3 expression only in LN-229 glioma cells (Fig. 1C). This
431 was also the cell line that exhibited the least potent pSMAD2 reduction after exposure to
432 ISTH1047 or ISTH0047 *in vitro* (Fig. 1F), supporting the notion that TGF-β_3 may

compensate for the loss of other isoforms to regulate TGF-β signaling (26). We therefore hypothesize that the effects of TGF-β isoform-specific inhibition on canonical and non-canonical pathways may be cell-dependent and do not solely rely on the basal expression of either TGF-β_1 or TGF-β_2 alone, but also on the potential availability of counter-regulatory pathways.

Exposure of glioma cells to ISTH1047 or ISTH0047 did not affect cell viability (Suppl. Fig. 4), although SMA-560 glioma cells transfected with the TGF-β_1-specfic ASO displayed reduced clonogenic survival, also resulting in lack of spheroid formation for assessment of invasive potential *in vitro* (Suppl. Fig. 4D). Ashley *et al*. (1998) also reported growth-suppressive properties of TGF-β_1 inhibition in SMA-560 cells and the induction of apoptosis, indicating a potential survival dependency of these cells specifically related to TGF-β_1 (35). Reduced migration and invasion of glioma cells upon TGF-β/SMAD singling blockade has been widely shown (12,14,36). Correlating with the greater pSMAD2 down-regulation after ASO-mediated TGF-β_1 or TGF-β_2 inhibition (Fig. 1D; Suppl Fig. 3C,D), these agents also exhibited more pronounced inhibitory effects on the migratory and invasive potential of glioma cells compared to TGF-βRI kinase inhibition (Fig. 2). The high binding affinity of LNA-modified ASO to cell surface proteins, such as heparin, can potentiate their cellular uptake via absorptive endocytosis and consequent target inhibition (37,38), and combined with the irreversible nature of ASO-mediated target silencing (39), may explain the superiority of these agents over small molecule ATP-competitive TGF-βR kinase inhibitors (12,40) observed here.

Since drug delivery to gliomas is one of the limiting factors of current novel therapeutic approaches administered systemically (41), we assessed whether these second-

456 generation ASO reach the tumor site after systemic treatment in orthotopic murine glioma
457 models *in vivo*. Indeed, systemic subcutaneous administration of DIG-labelled ISTH1047
458 resulted in a strong oligonucleotide accumulation in the tumors with minimal deposition in
459 the normal contralateral hemisphere (Fig. 3E). Even though *in vivo* oligonucleotide uptake
460 pathways are currently poorly understood, LNA modifications are known to improve the
461 pharmacokinetic properties of ASO, facilitating prolonged tissue half-life and more
462 efficient cellular uptake compared to AP12009 or other first generation ASO (18). The
463 only other approach to directly inhibit TGF-β ligand activity represents the intravenous
464 administration of the pan-TGF-β neutralizing antibody, 1D11 that also appears to
465 selectively accumulate in the tumor (15). Systemic treatment of glioma-bearing mice with
466 either of the two ASO molecules resulted in a ligand-specific down-regulation and
467 reduction of the SMAD-dependent target gene *PAI1* in the tumor-bearing hemisphere
468 (Fig. 3F,G). Given that *TGF-β_1* and *TGF-β_2* expression strongly correlate with *PAI1*
469 expression in The Cancer Genome Atlas (TCGA) analyses (6), this profound reduction in
470 *TGF-β* and *PAI1* levels demonstrates that isoform-specific targeting of TGF-β is feasible
471 and interferes with TGF-β signaling in the tumor following systemic administration. *TGF-*
472 *$\beta_{1/2}$* levels were up-regulated in the tumor compared to normal brain in both glioma models
473 (Fig. 3F) supporting the notion that *TGF-β* is highly expressed in glioblastoma (5,6).
474 However, we did not detect any increase in tumoral *TGF-β_2* compared to normal brain
475 tissue in SMA-560-bearing mice. The inherent low *TGF-β_2* expression levels of SMA-560
476 gliomas have been described before (13), which may not allow for the discrimination of
477 such changes at the mRNA level between tumoral and normal tissue. *TGF-β_2* levels in
478 SMA-560-bearing mice were reduced only after ISTH0047 treatment further supporting

479 the specificity and efficacy of these ASO in the glioma setting (Fig. 3F). Reduced *TGF-β$_1$*
480 or *TGF-β$_2$* levels resulted in a significant reduction of tumor invasiveness *in vivo* (Suppl.
481 Fig. 8), and are in line with our *in vitro* observations of reduced invasive potential (Fig.
482 2C,D), enhancing the importance of the TGF-β/SMAD pathway as a major mediator of
483 glioma cell invasion (12,42,43).
484 Based on these promising data, we determined the anti-glioma activity of both novel
485 antisense molecules *in vivo*. ISTH1047 or ISTH0047 treatment significantly reduced
486 tumor volumes and ultimately prolonged the survival of LN-308 or SMA-560 glioma-
487 bearing mice (Fig. 4A,B,G,H). Consistent with the *TGF-β* and *PAI1* mRNA inhibition data,
488 pSMAD2 levels were significantly reduced by ISTH1047 or ISTH0047 in both models (Fig.
489 5A,B,E,F). A recent study with the TGF-βRI antagonist, galunisertib, as monotherapy
490 showed a marginal survival benefit in the SMA-560 model, while it did not significantly
491 affect tumor size (13). Moreover, the 1D11 pan-TGF-β-neutralizing antibody resulted in
492 an almost complete tumor remission when administered daily in immunocompetent mice
493 bearing subcutaneous gliomas but, the opposite effect was noted when it was given to
494 immunodeficient glioma-bearing mice, additionally, 1D11 failed to show a therapeutic
495 effect in an orthotopic glioma model (15). Our ASO-mediated approach utilized a twice
496 weekly dosage regime after the initial 5-day ASO treatment and led to a striking decrease
497 of pSMAD2 levels and significant tumor size reduction in the xenogeneic LN-308-bearing
498 and the syngeneic SMA-560-bearing glioma models. In LN-229-bearing mice, a
499 significant survival benefit was only observed after ISTH0047 treatment without any
500 reduction in tumor burden which, however, was assessed at a very early point in time
501 which limits the significance of this finding (Fig. 4C,D). LN-229 gliomas exhibit a highly

invasive phenotype that could only be mitigated by ISTH0047-mediated *TGF-β$_2$* inhibition and not by ISTH1047 (Suppl. Fig. 8). Moreover, pSMAD2 expression was almost eliminated after ISTH0047 treatment suggesting that *TGF-β$_2$* inhibition has a potent effect on the *TGF-β* pathway in this model (Fig. 5C,D). Therefore, it may be that the survival benefit observed with ISTH0047 in this model is mainly due to the potent reduction of tumor infiltration and invasion (42), further supporting the cell-dependent effects of *TGF-β* isoform inhibition noted in our *in vitro* studies. We did not observe a significant survival benefit upon ASO treatment in the GIC model *in vivo*. However, *TGF-β$_2$* inhibition significantly reduced tumor volume and had the better survival outcome compared to *TGF-β$_1$* inhibition (Fig. 4E,F). In line with this finding, *TGF-β$_2$* is known to be an essential regulator of the self-renewing and tumor propagating capacity of patient-derived GIC (44). Therefore, a more intensive ISTH0047 treating regime has the potential to exert more prominent survival benefit in GIC tumor mouse models.

Since TGF-β is a multifunctional cytokine with major immunosuppressive properties, we assessed the host cell responses to ASO-mediated *TGF-β$_1$* or *TGF-β$_2$* inhibition in the syngeneic, immunocompetent SMA-560 glioma model. We noted enhanced immune cell infiltration in the tumor after ASO treatment. More specifically, the cytotoxic $CD45^+$ $CD8^+$ T-cell population was significantly increased after either ISTH1047 or ISTH0047 treatment (Fig. 6C). The enhanced tumor infiltration with cytotoxic T cells suggests that TGF-β depletion allows for an activation of the adaptive anti-tumor immune response. Interestingly, pSMAD2 depletion correlates with the increased tumoral cytotoxic T cell infiltration supporting the notion that targeting TGF-β signaling in tumors can restore immune surveillance (13,45). Finally, ISTH0047 treatment resulted in a significantly

reduced number of $CD31^+$ endothelial cells, suggesting that *TGF-β_2* inhibition may reduce the number of aberrant tumor blood vessels and thereby facilitate tumor vasculature normalization (13). Blood vessel normalization is a process associated with a better trafficking of immune cells in the tumoral bed, which may facilitate cytotoxic T cell infiltration (46). Overall, these data indicate a potential pro-immunogenic effect of ASO-mediated *TGF-$\beta_{1/2}$* inhibition that might assist in the elimination of glioma cells, while reducing their invasive and migratory abilities.

Except for ALAT levels marginally beyond the normal range upon treatment with ISTH1047, no relevant toxicity was observed in the *in vivo* survival experiments (Suppl. Fig. 10). However, when the two ASO molecules were administered as a combinatorial treatment in the syngeneic SMA-560 glioma model, the mice exhibited severe systemic toxicity and therefore this treatment arm was not selected for further investigations. For reasons currently undetermined, LNA-modified ASO have been linked with an increased risk of acute kidney injury in pre-clinical studies when compared to other second-generation ASO variants (47). However, *in vivo* pre-clinical toxicology studies tend to over-predict the renal effects of ASO, as these agents do not appear to exert significant nephrotoxicity when tested in humans (48). Therefore, even though informative, any toxicology studies performed in murine glioma models with ISTH1047 or ISTH0047 do not necessarily predict the situation in glioblastoma patients. Altogether, these data show that ASO-mediated TGF-β ligand targeting represents an alternative, convenient and efficient way to block the TGF-β/SMAD pathway resulting in a significant survival benefit compared to other approaches, in both the xenograft and syngeneic glioma setting *in vivo*.

The present dataset strongly suggests that TGF-β retains an important role in glioblastoma progression and that an efficient targeting approach can potentially improve clinical outcome. We show strong therapeutic activity of two novel second-generation TGF-β-specific ASO in two independent glioma models which may now allow for clinical evaluation of their therapeutic potential in human patients. Given the immune-modulatory activities of the two ASO molecules, a potential combination of ISTH1047 or ISTH0047 with immune checkpoint inhibitors that are currently explored in clinical neuro-oncology (49,50), may result in synergistic therapeutic activity and warrants further investigation.

Acknowledgments

We thank D. Mangani for help with the initial animal studies, and Julia Friesen and Franziska Wiget for the excellent technical assistance.

Funding

This study was supported by the Clinical Research Priority Program (CRPP) of the University of Zurich for the CRPP ImmunoCure and by a grant from the Swiss National Science Foundation (SNF 310030_170027) to PR.

Figure legends

Figure 1. ISTH1047 and ISTH0047 interfere with TGF-β signaling. A,**B**. LN-308 (**A**) or SMA-560 (**B**) glioma cells were exposed to ISTH1047 or ISTH0047 at 50 nM for 24 h and TGF-$\beta_{1/2}$ protein levels in the cell culture supernatant were determined by ELISA at 48, 72 or 96 h post transfection. **C**. LN-308, LN-229, ZH-161 or SMA-560 glioma cells were exposed to ISTH1047 or ISTH0047 at 50 nM for 24 h and *TGF-$\beta_{1/2/3}$* mRNA levels were assessed by RT-PCR 48 h post transfection. **D,E**. LN-308 or SMA-560 glioma cells were exposed to ISTH1047 or ISTH0047 at 50 nM for 24 h. pSMAD2 (**D**), pSMAD3, total SMAD3, pAKT and total AKT (**E**) levels were assessed by immunoblot at 48 h post transfection. **F**. LN-229 or ZH-161 glioma cells were exposed to ISTH1047 or ISTH0047 at 50 nM for 24 h. pSMAD2, total SMAD2, pSMAD3, total SMAD3, pAKT and total AKT levels were assessed by immunoblot at 48 h post transfection. C3_ISTH0047 at 50 nM was used as scrambled sequence oligonucleotide control (Ctrl). Exogenous TGF-$\beta_{1/2}$ (5 ng/ml) was used to induce pSMAD2 in ZH-161. The TGF-β receptor I kinase inhibitor SD-208 (1 µM) was used as an additional control for TGF-β pathway inhibition. Results are expressed as means and SD (n=3), statistical analysis was performed with one-way ANOVA and Bonferroni post-hoc testing (*$p < 0.05$, ** $p < 0.01$).

Figure 2. TGF-β inhibition by ISTH1047 or ISTH0047 reduces glioma cell migration and invasion. A,**B**. LN-308 (**A**) or SMA-560 (**B**) glioma cells were transfected with ISTH1047, ISTH0047, control oligonucleotide (Ctrl) or exposed to galunisertib, SD-208 or recombinant TGF-$\beta_{1/2}$ at the indicated concentrations for 72 h and then examined in Transwell-Boyden chamber assays. Data are expressed as mean migrated cells per

membrane. **C**,**D**. LN-308 (**C**) or SMA-560 (**D**) glioma cells transfected with 50 nM ISTH1047 or ISTH0047, exposed to 1 µM SD-208, 5 ng/ml TGF-β_1 or 5 ng/ml TGF-β_2 for 24 h were allowed to form spheroids in agar and seeded in collagen-I. Invasion was assessed by quantifying the area of invaded cells into the collagen over 96 h. Results are expressed as means and SD (n=3), statistical analysis was performed with one-way ANOVA and Bonferroni post-hoc testing (*$p < 0.05$).

Figure 3. ASO are detected at the tumor site upon systemic administration and inhibit *TGF-β1* or *TGF-β2* expression in orthotopically growing gliomas *in vivo*. LN-308 (10^5) or SMA-560 ($5x10^3$) glioma cells were injected stereotactically into the right hemisphere of Crl: CD1 Foxn1 or VM/Dk mice, respectively. **A-E**. Twenty-five or five days after tumor inoculation for Crl: CD1 Foxn1 or VM/Dk mice, respectively, systemic treatment with DIG-ISTH1047 (10 mg/kg) was initiated for 5 consecutive days. Two days following the last injection, brains from LN-308 (**A**) or SMA-560 (**B**) glioma-bearing mice were collected and histologically assessed for DIG expression in the tumor region using an anti-mouse DIG antibody. Representative images of DIG fluorescence staining in LN-308 (**A**) or SMA-560 (**B**) tumors are shown (DIG, green; nuclei staining with DAPI, blue). Contralateral normal brain hemisphere was used as additional control (**C**). Mouse IgG was used as a negative control (**D**). Mean fluorescence intensity was quantified using the Bitplane Imaris software (**E**). Results are expressed as means and SD (n=3), statistical analysis was performed with one-way ANOVA and Bonferroni post-hoc testing (*$p < 0.05$, ** $p < 0.01$). **F**, **G**. Twenty-five or five days after tumor inoculation for Crl: CD1 Foxn1 or VM/Dk mice, respectively, systemic treatment with C3_ISTH0047 (Ctrl) (20 mg/kg),

ISTH1047 (10 mg/kg) or ISTH0047 (20 mg/kg) was initiated for 5 consecutive days. Two days following the last injection, tumor- and non-tumor-bearing (normal) hemispheres from LN-308 or SMA-560 glioma-bearing mice were collected and assessed for *TGF-β$_1$*, *TGF-β$_2$*, *TGF-β$_3$* or *PAI1* mRNA expression using RT-qPCR. Human-specific *TGF-β$_1$*, *TGF-β$_2$*, *TGF-β$_3$* or *PAI1* primer sequences were used to assess target gene expression in LN-308-derived tumors. Results are expressed as means and SD (n=4), statistical analysis was performed with one-way ANOVA and Bonferroni post-hoc testing ($p < 0.05$; * = control vs treatment in tumor tissue; $^{+}$ = control vs treatment in normal tissue; $^{\#}$ = normal tissue vs. tumor tissue).

Figure 4. Systemic treatment of glioma-bearing mice with ISTH1047 or ISTH0047 inhibits tumor growth and prolongs survival. A-H. LN-308 (10^5), LN-229 (10^5), ZH-161 (10^5) or SMA-560 ($5x10^3$) glioma cells were injected stereotactically into the right hemisphere of Crl: CD1 Foxn1 or VM/Dk mice, respectively. Twenty-five (LN-308), ten (LN-229, ZH-161) or five days (SMA-560) after tumor inoculation, systemic treatment with C3_ISTH0047 (Ctrl) (20 mg/kg), ISTH1047 (10 mg/kg) or ISTH0047 (20 mg/kg) was initiated for 5 consecutive days. Agents were administered twice weekly thereafter. Mice were sacrificed when they developed grade 2 neurological symptoms. Survival curves for LN-308 (**A**), LN-229 (**C**), ZH-161 (**E**) and SMA-560 (**G**) were analyzed for differences via log-rank (Martel-Cox) test at $^{*}p < 0.05$ and $^{**}p < 0.01$. Brains from three pre-randomized LN-308 (**B**), LN-229 (**D**), ZH-161 (**F**) or SMA-560 (**H**) glioma-bearing mice per group were subjected to for histological analyses when the first mouse developed clinical symptoms. Tumor volumes were determined using the ellipsoid geometric primitive formula. Results

(**B**,**D,F,H**) are expressed as means and SD (n=3), statistical analysis was performed with one-way ANOVA and Bonferroni post-hoc testing (*$p < 0.05$).

Figure 5. ISTH1047 or ISTH0047 treatment reduces tumoral SMAD2 phosphorylation. A-F. LN-308 (10^5), LN-229 (10^5) or SMA-560 ($5x10^3$) glioma cells were injected stereotactically into the right hemisphere of Crl: CD1 Foxn1 or VM/Dk mice, respectively. Twenty-five (LN-308), ten (LN-229) or five days (SMA-560) after tumor inoculation, systemic treatment with C3_ISTH0047 (Ctrl) (20 mg/kg), ISTH1047 (10 mg/kg) or ISTH0047 (20 mg/kg) was initiated for 5 consecutive days and then administered twice weekly. Brains from LN-308 (**A,B**), LN-229 (**C,D**) or SMA-560 (**E,F**) glioma-bearing mice were extracted for histological analyses from three pre-randomized animals per group when the first mouse developed clinical symptoms to assess pSMAD2 levels. Representative images of pSMAD2 stainings of LN-308 (**A**), LN-229 (**C**) or SMA-560-derived (**E**) tumors are shown (pSMAD2, green; nuclei staining with DAPI, blue). Mean fluorescence intensity (**B,D,F**) was quantified using the Bitplane Imaris software. Results (**B,D,F**) are expressed as means and SD (n=2-3), statistical analysis was performed with one-way ANOVA and Bonferroni post-hoc testing (*$p < 0.05$).

Figure 6. Modulation of tumor immune cell infiltration in ISTH1047- or ISTH0047-treated syngeneic SMA-560-bearing mice. A-E. SMA-560 ($5x10^3$) glioma cells were injected stereotactically into the right hemisphere of VM/Dk mice. Five days after tumor inoculation, systemic treatment with C3_ISTH0047 (Ctrl) (20 mg/kg), ISTH1047 (10 mg/kg) or ISTH0047 (20 mg/kg) was initiated for 5 consecutive days and then

administered twice weekly. Brains from glioma-bearing mice were extracted for histological analyses from three pre-randomized animals per group when the first mouse developed clinical symptoms to detect $CD45^+$ leukocyte (**A**), $CD3^+$ T cell (**B**), $CD8^+$ cytotoxic T cell (**C**), $CD4^+$ T helper cell (**D**) or $CD11b^+$ monocyte/microglia (**E**) populations. Results are expressed as means and SD (n=12), statistical analysis was performed with one-way ANOVA and Bonferroni post-hoc testing (*$p < 0.05$, ** $p < 0.01$).

References

1. Weller M, van den Bent M, Tonn JC, Stupp R, Preusser M, Cohen-Jonathan-Moyal E*, et al.* European Association for Neuro-Oncology (EANO) guideline on the diagnosis and treatment of adult astrocytic and oligodendroglial gliomas. The Lancet Oncology **2017**;18(6):e315-e29.
2. Hinck AP. Structural studies of the TGF-betas and their receptors - insights into evolution of the TGF-beta superfamily. FEBS letters **2012**;586(14):1860-70.
3. Massague J. TGF[beta] signalling in context. Nat Rev Mol Cell Biol **2012**;13(10):616-30.
4. Pickup M, Novitskiy S, Moses HL. The roles of TGF[beta] in the tumour microenvironment. Nat Rev Cancer **2013**;13(11):788-99.
5. Bruna A, Darken RS, Rojo F, Ocana A, Penuelas S, Arias A*, et al.* High TGFbeta-Smad activity confers poor prognosis in glioma patients and promotes cell proliferation depending on the methylation of the PDGF-B gene. Cancer Cell **2007**;11(2):147-60.
6. Frei K, Gramatzki D, Tritschler I, Schroeder JJ, Espinoza L, Rushing EJ*, et al.* Transforming growth factor-beta pathway activity in glioblastoma. Oncotarget **2015**;6(8):5963-77.
7. Hardee ME, Marciscano AE, Medina-Ramirez CM, Zagzag D, Narayana A, Lonning SM*, et al.* Resistance of glioblastoma-initiating cells to radiation mediated by the tumor microenvironment can be abolished by inhibiting transforming growth factor-beta. Cancer Res **2012**;72(16):4119-29.
8. Liu S, Sun J, Lan Q. TGF-beta-induced miR10a/b expression promotes human glioma cell migration by targeting PTEN. Molecular medicine reports **2013**;8(6):1741-6.
9. Stander M, Naumann U, Dumitrescu L, Heneka M, Loschmann P, Gulbins E*, et al.* Decorin gene transfer-mediated suppression of TGF-beta synthesis abrogates experimental malignant glioma growth in vivo. Gene therapy **1998**;5(9):1187-94.

10. Ventura E, Weller M, Burghardt I. Cutting Edge: ERK1 Mediates the Autocrine Positive Feedback Loop of TGF-beta and Furin in Glioma-Initiating Cells. Journal of immunology (Baltimore, Md : 1950) **2017**;198(12):4569-74.

11. Roth P, Silginer M, Goodman SL, Hasenbach K, Thies S, Maurer G*, et al.* Integrin control of the transforming growth factor-beta pathway in glioblastoma. Brain : a journal of neurology **2013**;136(Pt 2):564-76.

12. Uhl M, Aulwurm S, Wischhusen J, Weiler M, Ma JY, Almirez R*, et al.* SD-208, a novel transforming growth factor beta receptor I kinase inhibitor, inhibits growth and invasiveness and enhances immunogenicity of murine and human glioma cells in vitro and in vivo. Cancer Res **2004**;64(21):7954-61.

13. Mangani D, Weller M, Seyed Sadr E, Willscher E, Seystahl K, Reifenberger G*, et al.* Limited role for transforming growth factor-beta pathway activation-mediated escape from VEGF inhibition in murine glioma models. Neuro Oncol **2016**;18(12):1610-21.

14. Zhang M, Kleber S, Rohrich M, Timke C, Han N, Tuettenberg J*, et al.* Blockade of TGF-beta signaling by the TGFbetaR-I kinase inhibitor LY2109761 enhances radiation response and prolongs survival in glioblastoma. Cancer Res **2011**;71(23):7155-67.

15. Hulper P, Schulz-Schaeffer W, Dullin C, Hoffmann P, Harper J, Kurtzberg L*, et al.* Tumor localization of an anti-TGF-beta antibody and its effects on gliomas. International journal of oncology **2011**;38(1):51-9.

16. Brandes AA, Carpentier AF, Kesari S, Sepulveda-Sanchez JM, Wheeler HR, Chinot O*, et al.* A Phase II randomized study of galunisertib monotherapy or galunisertib plus lomustine compared with lomustine monotherapy in patients with recurrent glioblastoma. Neuro Oncol **2016**;18(8):1146-56.

17. Rodon J, Carducci MA, Sepulveda-Sanchez JM, Azaro A, Calvo E, Seoane J*, et al.* First-in-human dose study of the novel transforming growth factor-beta receptor I kinase inhibitor LY2157299 monohydrate in patients with advanced cancer and glioma. Clinical

cancer research : an official journal of the American Association for Cancer Research **2015**;21(3):553-60.

18. Khorkova O, Wahlestedt C. Oligonucleotide therapies for disorders of the nervous system. Nat Biotech **2017**;35(3):249-63.

19. Moreno PMD, Pêgo AP. Therapeutic antisense oligonucleotides against cancer: hurdling to the clinic. Frontiers in Chemistry **2014**;2:87.

20. Bogdahn U, Hau P, Stockhammer G, Venkataramana NK, Mahapatra AK, Suri A*, et al.* Targeted therapy for high-grade glioma with the TGF-beta2 inhibitor trabedersen: results of a randomized and controlled phase IIb study. Neuro Oncol **2011**;13(1):132-42.

21. Evers MM, Toonen LJA, van Roon-Mom WMC. Antisense oligonucleotides in therapy for neurodegenerative disorders. Advanced Drug Delivery Reviews **2015**;87:90-103.

22. Wahlestedt C, Salmi P, Good L, Kela J, Johnsson T, Hokfelt T*, et al.* Potent and nontoxic antisense oligonucleotides containing locked nucleic acids. Proceedings of the National Academy of Sciences of the United States of America **2000**;97(10):5633-8.

23. Serano RD, Pegram CN, Bigner DD. Tumorigenic cell culture lines from a spontaneous VM/Dk murine astrocytoma (SMA). Acta neuropathologica **1980**;51(1):53-64.

24. Le Rhun E, von Achenbach C, Lohmann B, Silginer M, Schneider H, Meetze K*, et al.* Profound, durable and MGMT-independent sensitivity of glioblastoma cells to cyclin-dependent kinase inhibition. International journal of cancer **2019**;145(1):242-53.

25. Silginer M, Burghardt I, Gramatzki D, Bunse L, Leske H, Rushing EJ*, et al.* The aryl hydrocarbon receptor links integrin signaling to the TGF-beta pathway. Oncogene **2016**;35(25):3260-71.

26. Seystahl K, Papachristodoulou A, Burghardt I, Schneider H, Hasenbach K, Janicot M*, et al.* Biological Role and Therapeutic Targeting of TGF-beta3 in Glioblastoma. Mol Cancer Ther **2017**;16(6):1177-86.

27. Akiyoshi S, Ishii M, Nemoto N, Kawabata M, Aburatani H, Miyazono K. Targets of transcriptional regulation by transforming growth factor-beta: Expression profile analysis using oligonucleotide arrays. Jpn J Cancer Res **2001**;92(3):257-68.

28. Vester B, Wengel J. LNA (locked nucleic acid): high-affinity targeting of complementary RNA and DNA. Biochemistry **2004**;43(42):13233-41.

29. Hau P, Jachimczak P, Schlingensiepen R, Schulmeyer F, Jauch T, Steinbrecher A*, et al.* Inhibition of TGF-beta 2 with AP 12009 in recurrent malignant gliomas: From preclinical to phase I/II studies. Oligonucleotides **2007**;17(2):201-12.

30. Naumann U, Maass P, Gleske AK, Aulwurm S, Weller M, Eisele G. Glioma gene therapy with soluble transforming growth factor-beta receptors II and III. International journal of oncology **2008**;33(4):759-65.

31. Guerrero PA, Tchaicha JH, Chen Z, Morales JE, McCarty N, Wang Q*, et al.* Glioblastoma stem cells exploit the alphavbeta8 integrin-TGFbeta1 signaling axis to drive tumor initiation and progression. Oncogene **2017**;36(47):6568-80.

32. Zhang K, Liu X, Hao F, Dong A, Chen D. Targeting TGF-beta1 inhibits invasion of anaplastic thyroid carcinoma cell through SMAD2-dependent S100A4-MMP-2/9 signalling. American journal of translational research **2016**;8(5):2196-209.

33. Yin Q, Liu S, Dong A, Mi X, Hao F, Zhang K. Targeting Transforming Growth Factor-Beta1 (TGF-beta1) Inhibits Tumorigenesis of Anaplastic Thyroid Carcinoma Cells Through ERK1/2-NFkappakB-PUMA Signaling. Medical science monitor : international medical journal of experimental and clinical research **2016**;22:2267-77.

34. O'Reilly MA, Danielpour D, Roberts AB, Sporn MB. Regulation of Expression of Transforming Growth Factor-β2 by Transforming Growth Factor-β Isoforms is Dependent upon Cell Type. Growth Factors **1992**;6(4):193-201.

35. Ashley DM, Sampson JH, Archer GE, Hale LP, Bigner DD. Local production of TGF beta1 inhibits cerebral edema, enhances TNF-alpha induced apoptosis and improves survival in a murine glioma model. Journal of neuroimmunology **1998**;86(1):46-52.

36. Hau P, Jachimczak P, Bogdahn U. Treatment of malignant gliomas with TGF-beta2 antisense oligonucleotides. Expert review of anticancer therapy **2009**;9(11):1663-74.

37. Sirois CM, Jin T, Miller AL, Bertheloot D, Nakamura H, Horvath GL*, et al.* RAGE is a nucleic acid receptor that promotes inflammatory responses to DNA. The Journal of experimental medicine **2013**;210(11):2447-63.

38. Juliano RL, Ming X, Nakagawa O. Cellular uptake and intracellular trafficking of antisense and siRNA oligonucleotides. Bioconjugate chemistry **2012**;23(2):147-57.

39. Lundin KE, Gissberg O, Smith CIE. Oligonucleotide Therapies: The Past and the Present. Human Gene Therapy **2015**;26(8):475-85.

40. Herbertz S, Sawyer JS, Stauber AJ, Gueorguieva I, Driscoll KE, Estrem ST*, et al.* Clinical development of galunisertib (LY2157299 monohydrate), a small molecule inhibitor of transforming growth factor-beta signaling pathway. Drug Design, Development and Therapy **2015**;9:4479-99.

41. van Tellingen O, Yetkin-Arik B, de Gooijer MC, Wesseling P, Wurdinger T, de Vries HE. Overcoming the blood-brain tumor barrier for effective glioblastoma treatment. Drug resistance updates : reviews and commentaries in antimicrobial and anticancer chemotherapy **2015**;19:1-12.

42. Tran TT, Uhl M, Ma JY, Janssen L, Sriram V, Aulwurm S*, et al.* Inhibiting TGF-beta signaling restores immune surveillance in the SMA-560 glioma model. Neuro Oncol **2007**;9(3):259-70.

43. Tchaicha JH, Reyes SB, Shin J, Hossain MG, Lang FF, McCarty JH. Glioblastoma angiogenesis and tumor cell invasiveness are differentially regulated by beta8 integrin. Cancer Res **2011**;71(20):6371-81.

44. Penuelas S, Anido J, Prieto-Sanchez RM, Folch G, Barba I, Cuartas I*, et al.* TGF-beta increases glioma-initiating cell self-renewal through the induction of LIF in human glioblastoma. Cancer Cell **2009**;15(4):315-27.

45. Rich JN. The role of transforming growth factor-beta in primary brain tumors. Front Biosci **2003**;8:e245-60.

46. Liu J, Liao S, Diop-Frimpong B, Chen W, Goel S, Naxerova K*, et al.* TGF-beta blockade improves the distribution and efficacy of therapeutics in breast carcinoma by normalizing the tumor stroma. Proceedings of the National Academy of Sciences of the United States of America **2012**;109(41):16618-23.

47. Engelhardt JA. Comparative Renal Toxicopathology of Antisense Oligonucleotides. Nucleic acid therapeutics **2016**;26(4):199-209.

48. Crooke ST, Baker BF, Kwoh TJ, Cheng W, Schulz DJ, Xia S*, et al.* Integrated Safety Assessment of 2′-O-Methoxyethyl Chimeric Antisense Oligonucleotides in NonHuman Primates and Healthy Human Volunteers. Molecular Therapy **2016**;24(10):1771-82.

49. Bouffet E, Larouche V, Campbell BB, Merico D, de Borja R, Aronson M*, et al.* Immune Checkpoint Inhibition for Hypermutant Glioblastoma Multiforme Resulting From Germline Biallelic Mismatch Repair Deficiency. J Clin Oncol **2016**;34(19):2206-11.

50. Weller M, Roth P, Preusser M, Wick W, Reardon DA, Platten M*, et al.* Vaccine-based immunotherapeutic approaches to gliomas and beyond. Nature reviews Neurology **2017**;13(6):363-74.

Figure 1

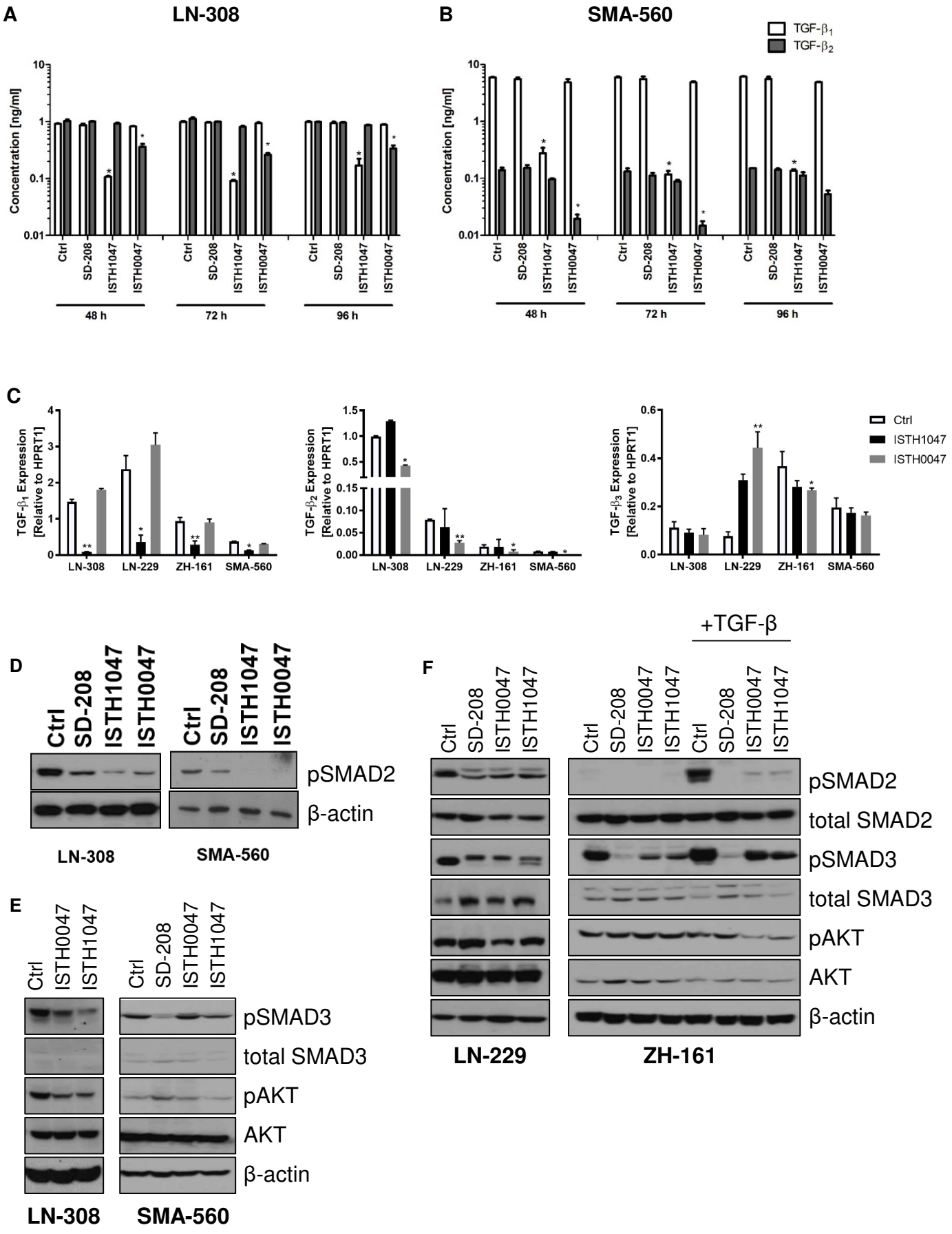
A
LN-308
B
SMA-560
TGF-β1
TGF-β2
Concentration [ng/ml]
Ctrl
SD-208
ISTH1047
ISTH0047
48 h
72 h
96 h
C
TGF-β1 Expression [Relative to HPRT1]
TGF-β2 Expression [Relative to HPRT1]
TGF-β3 Expression [Relative to HPRT1]
LN-308
LN-229
ZH-161
SMA-560
Ctrl
ISTH1047
ISTH0047
D
pSMAD2
β-actin
LN-308
SMA-560
E
pSMAD3
total SMAD3
pAKT
AKT
β-actin
LN-308
SMA-560
F
+TGF-β
pSMAD2
total SMAD2
pSMAD3
total SMAD3
pAKT
AKT
β-actin
LN-229
ZH-161

Figure 2

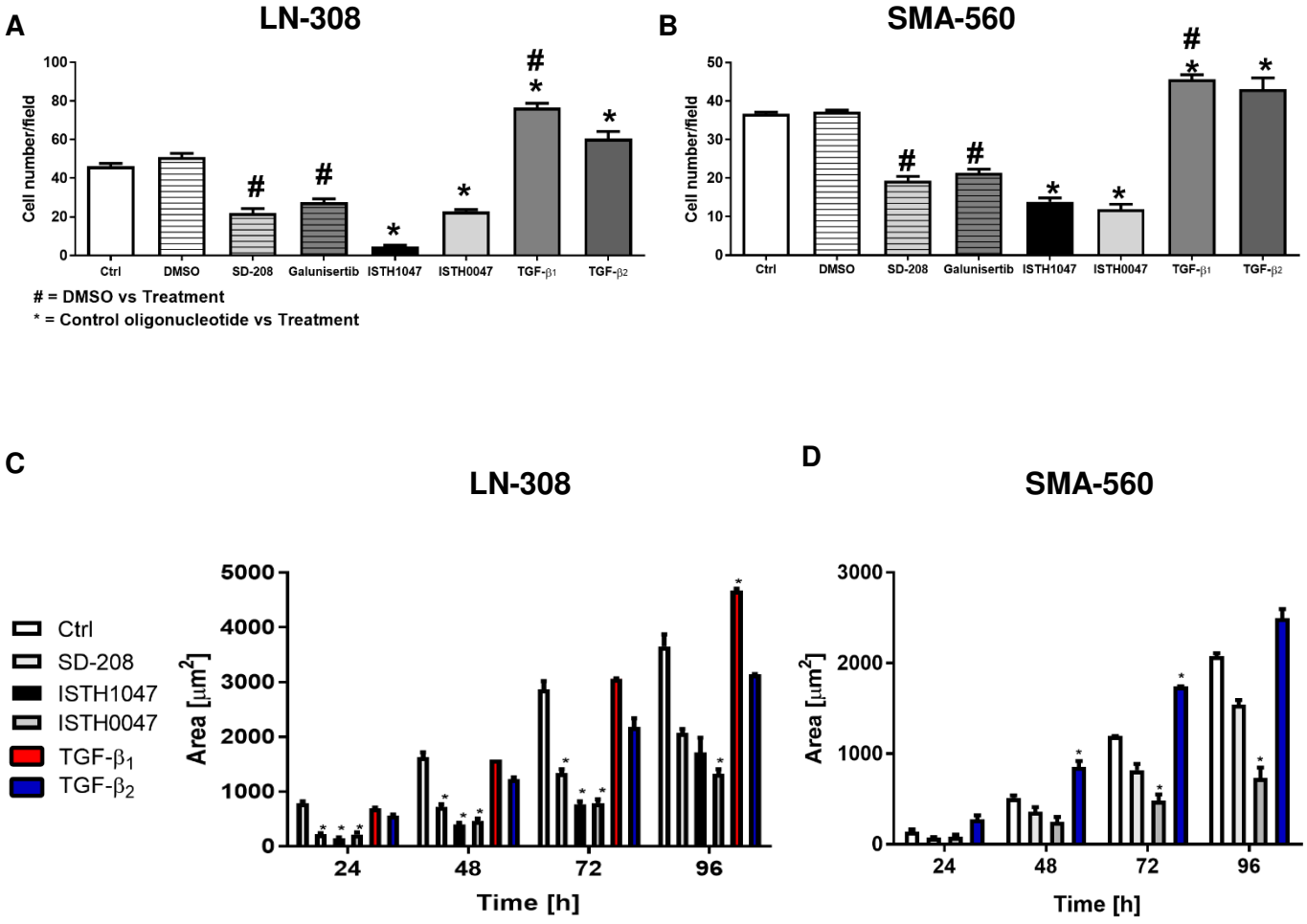
A
LN-308
Cell number/field
Ctrl
DMSO
SD-208
Galunisertib
ISTH1047
ISTH0047
TGF-β1
TGF-β2
= DMSO vs Treatment
* = Control oligonucleotide vs Treatment
B
SMA-560
C
LN-308
Area [μm²]
Time [h]
D
SMA-560

Figure 3

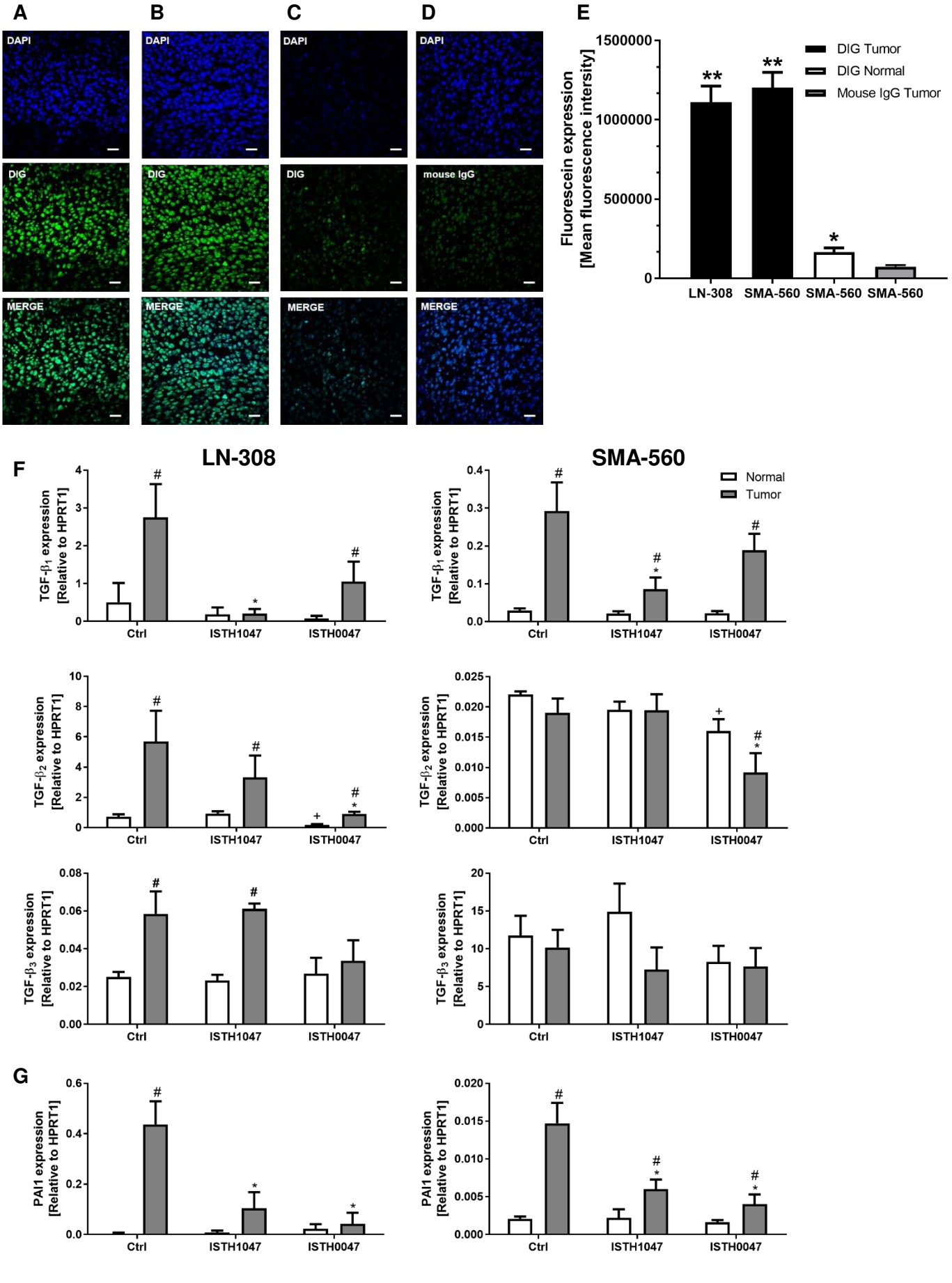
A
B
C
D
DAPI
DIG
mouse IgG
MERGE
E
Fluorescein expression [Mean fluorescence intersity]
1500000
1000000
500000
0
DIG Tumor
DIG Normal
Mouse IgG Tumor
LN-308
SMA-560
SMA-560
SMA-560
F
LN-308
SMA-560
Normal
Tumor
TGF-β1 expression [Relative to HPRT1]
TGF-β2 expression [Relative to HPRT1]
TGF-β3 expression [Relative to HPRT1]
Ctrl
ISTH1047
ISTH0047
G
PAI1 expression [Relative to HPRT1]

Figure 4

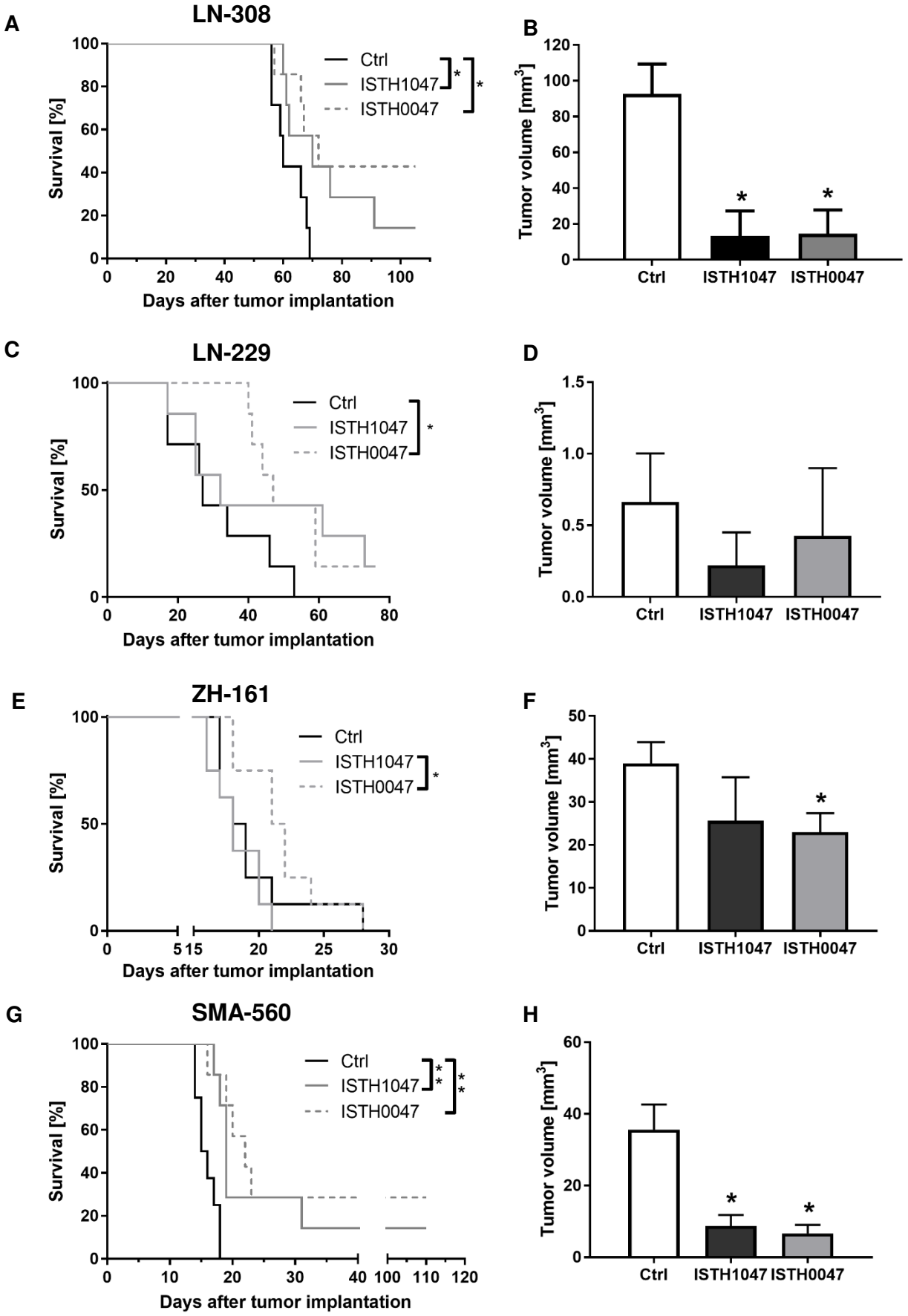
A
LN-308
Survival [%]
Days after tumor implantation
Ctrl
ISTH1047
ISTH0047
B
Tumor volume [mm3]
Ctrl
ISTH1047
ISTH0047
C
LN-229
Survival [%]
Days after tumor implantation
Ctrl
ISTH1047
ISTH0047
D
Tumor volume [mm3]
Ctrl
ISTH1047
ISTH0047
E
ZH-161
Survival [%]
Days after tumor implantation
Ctrl
ISTH1047
ISTH0047
F
Tumor volume [mm3]
Ctrl
ISTH1047
ISTH0047
G
SMA-560
Survival [%]
Days after tumor implantation
Ctrl
ISTH1047
ISTH0047
H
Tumor volume [mm3]
Ctrl
ISTH1047
ISTH0047

Figure 5

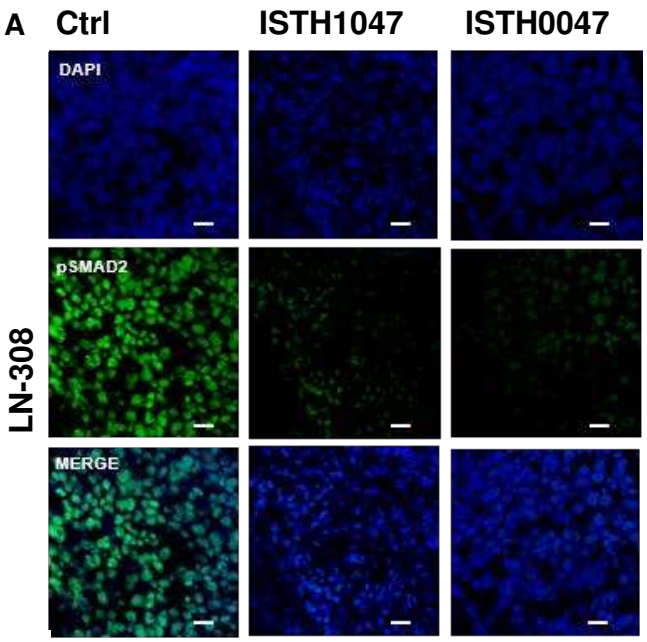
A
Ctrl
ISTH1047
ISTH0047
DAPI
pSMAD2
MERGE
LN-308

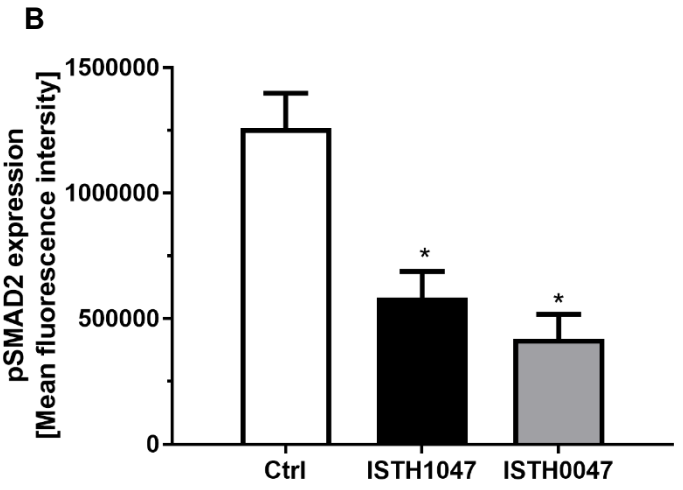
B
pSMAD2 expression
[Mean fluorescence intersity]
1500000
1000000
500000
0
*
*
Ctrl
ISTH1047
ISTH0047

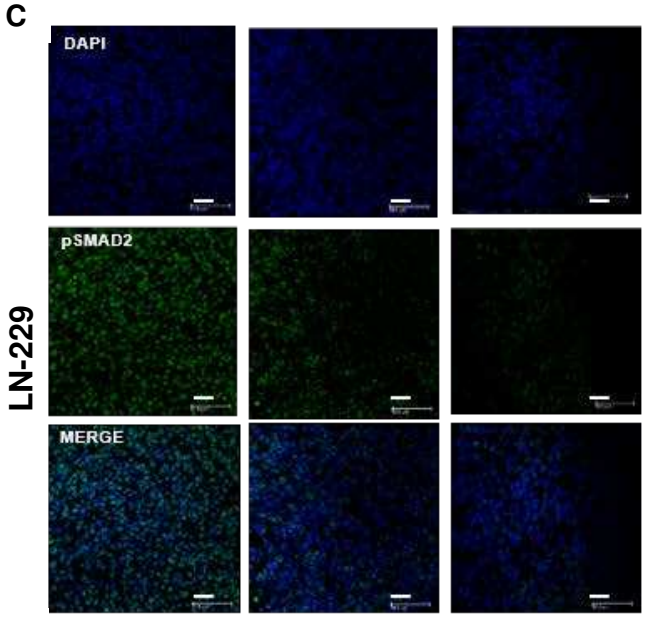
C
DAPI
pSMAD2
MERGE
LN-229

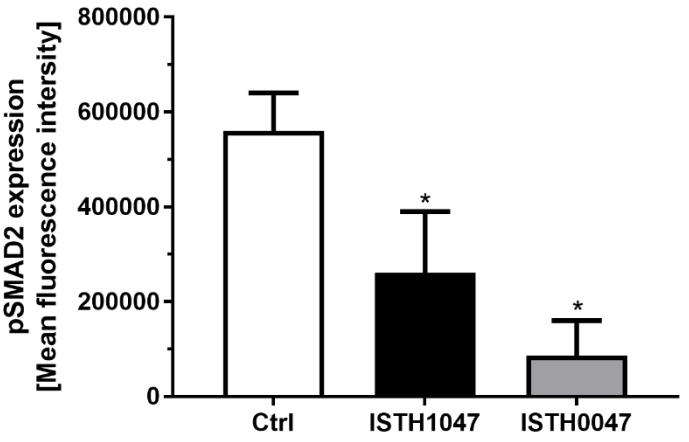
D
pSMAD2 expression
[Mean fluorescence intersity]
800000
600000
400000
200000
0
*
*
Ctrl
ISTH1047
ISTH0047

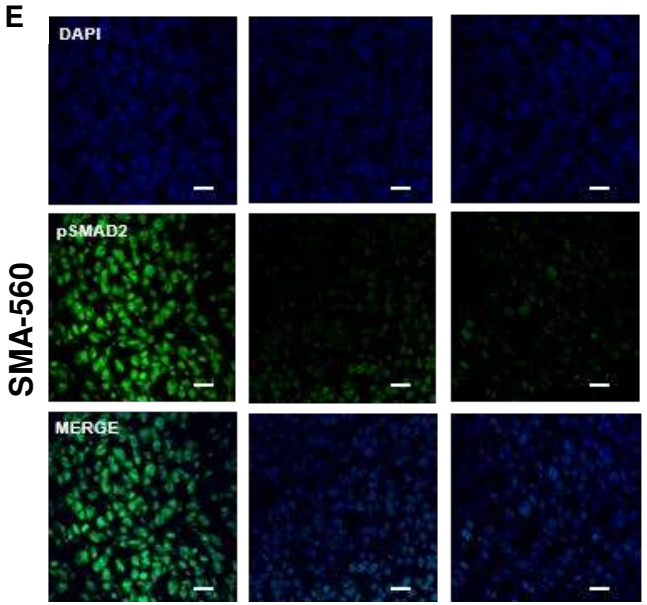
E
DAPI
pSMAD2
MERGE
SMA-560

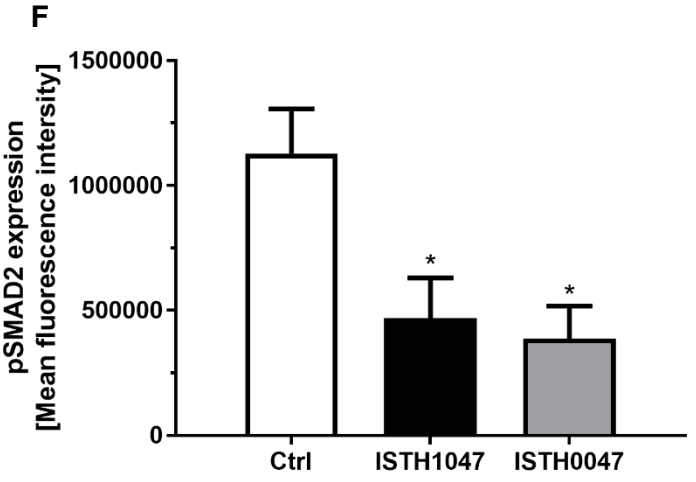
F
pSMAD2 expression
[Mean fluorescence intersity]
1500000
1000000
500000
0
*
*
Ctrl
ISTH1047
ISTH0047

Figure 6

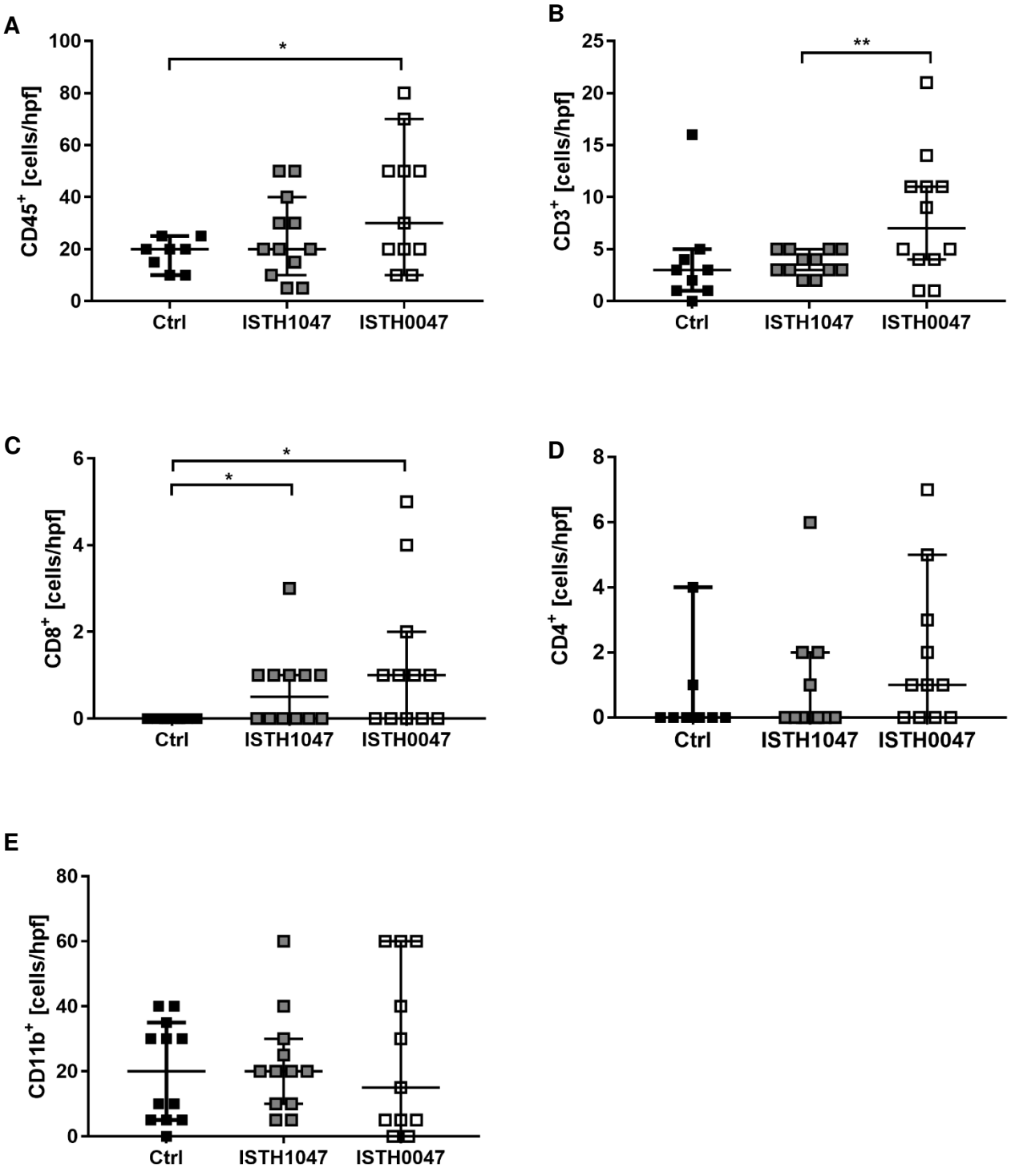
A
CD45+ [cells/hpf]
100
80
60
40
20
0
*
Ctrl
ISTH1047
ISTH0047
B
CD3+ [cells/hpf]
25
20
15
10
5
0
**
Ctrl
ISTH1047
ISTH0047
C
CD8+ [cells/hpf]
6
4
2
0
*
*
Ctrl
ISTH1047
ISTH0047
D
CD4+ [cells/hpf]
8
6
4
2
0
Ctrl
ISTH1047
ISTH0047
E
CD11b+ [cells/hpf]
80
60
40
20
0
Ctrl
ISTH1047
ISTH0047

Supplementary Figure 1

A ISTH1047: 5´TCGATGCGCTTCCG-3´

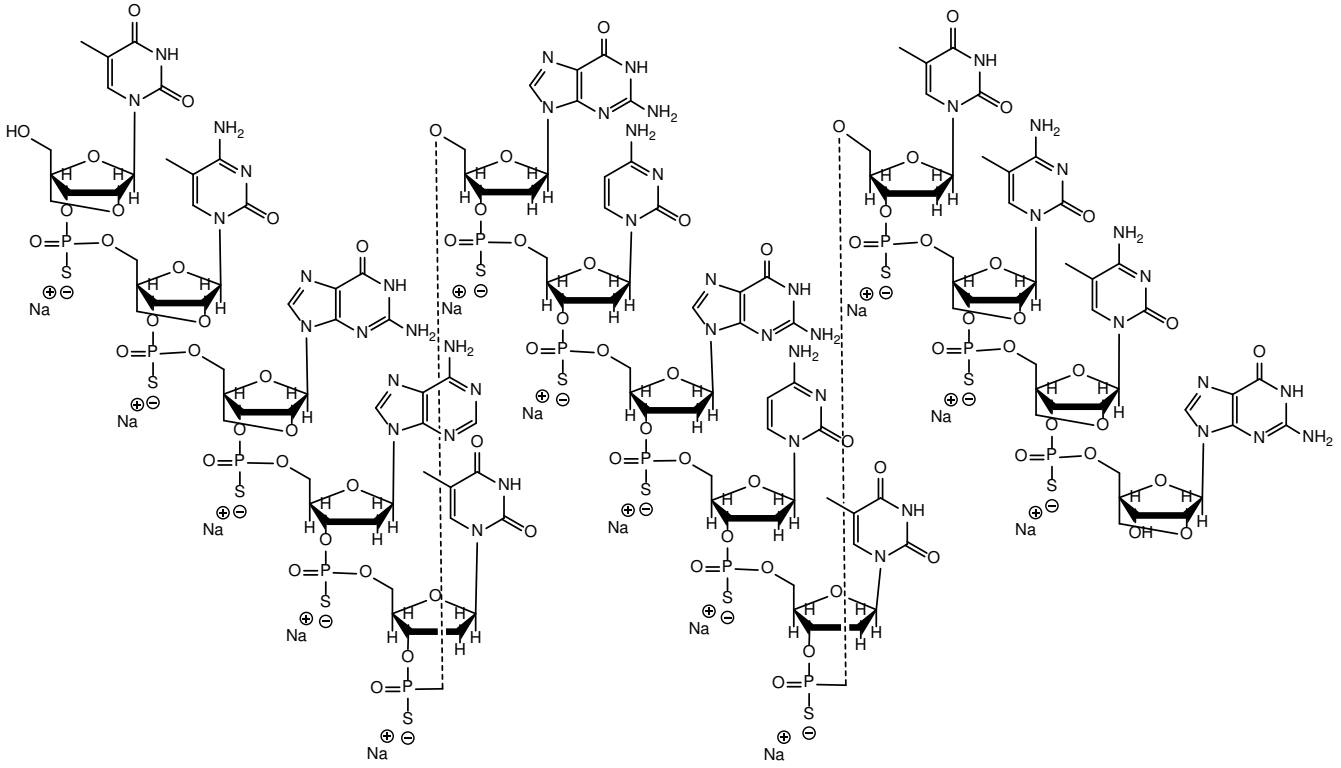

B ISTH0047: 5´CAAAGTATTTGGTCTCC-3´

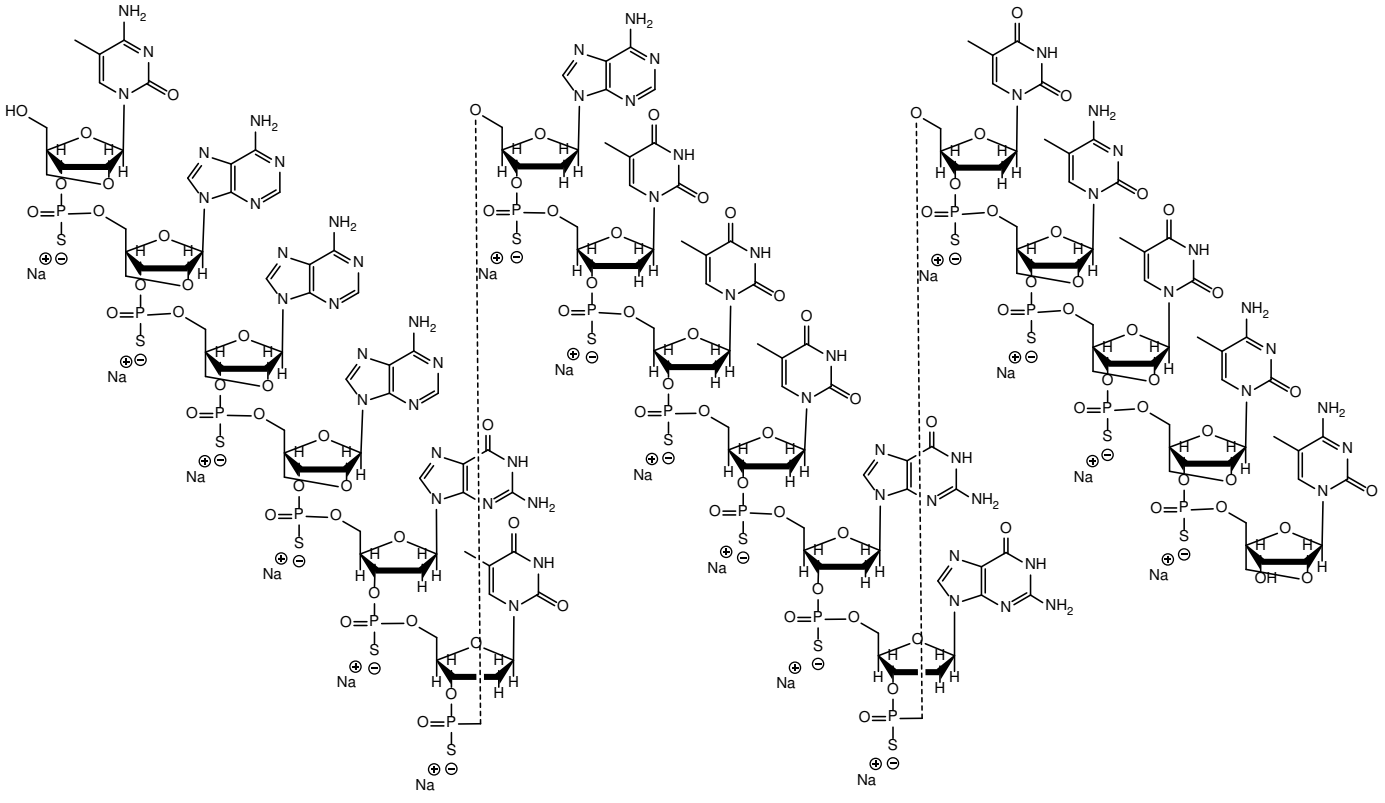

Supplementary Figure 2

A ISTH1047: 5´TCGATGCGCTTCCG-3´

Homo sapiens transforming growth factor beta 1 (TGFB1), mRNA

Sequence ID: NM_000660.6 **Length:** 2741 **Number of Matches:** 1

Range 1: 966 to 979 GenBank Graphics Next Match Previous Match

Score	Expect	Identities	Gaps	Strand
28.2 bits(14)	24	14/14(100%)	0/14(0%)	Plus/Minus

```
Query  1    TCGATGCGCTTCCG  14
           ||||||||||||||
Sbjct  979  TCGATGCGCTTCCG  966
```

Mus musculus transforming growth factor, beta 1 (Tgfb1), mRNA

Sequence ID: NM_011577.2 **Length:** 2191 **Number of Matches:** 1

Range 1: 994 to 1007 GenBank Graphics Next Match Previous Match

Score	Expect	Identities	Gaps	Strand
28.2 bits(14)	20	14/14(100%)	0/14(0%)	Plus/Minus

```
Query  1     TCGATGCGCTTCCG  14
            ||||||||||||||
Sbjct  1007  TCGATGCGCTTCCG  994
```

B ISTH0047: 5´CAAAGTATTTGGTCTCC-3´

Homo sapiens transforming growth factor beta 2 (TGFB2), transcript variant 1, mRNA

Sequence ID: NM_001135599.3 **Length:** 6016 **Number of Matches:** 1

Range 1: 3284 to 3300 GenBank Graphics Next Match Previous Match

Score	Expect	Identities	Gaps	Strand
34.2 bits(17)	0.39	17/17(100%)	0/17(0%)	Plus/Minus

```
Query  1     CAAAGTATTTGGTCTCC  17
            |||||||||||||||||
Sbjct  3300  CAAAGTATTTGGTCTCC  3284
```

Mus musculus transforming growth factor, beta 2 (Tgfb2), mRNA

Sequence ID: NM_009367.3 **Length:** 4725 **Number of Matches:** 1

Range 1: 3029 to 3045 GenBank Graphics Next Match Previous Match

Score	Expect	Identities	Gaps	Strand
34.2 bits(17)	0.32	17/17(100%)	0/17(0%)	Plus/Minus

```
Query  1     CAAAGTATTTGGTCTCC  17
            |||||||||||||||||
Sbjct  3045  CAAAGTATTTGGTCTCC  3029
```

*Source: https://blast.ncbi.nlm.nih.gov/Blast.cgi?PROGRAM=blastn&PAGE_TYPE=BlastSearch&LINK_LOC=blasthome

Supplementary Figure 3

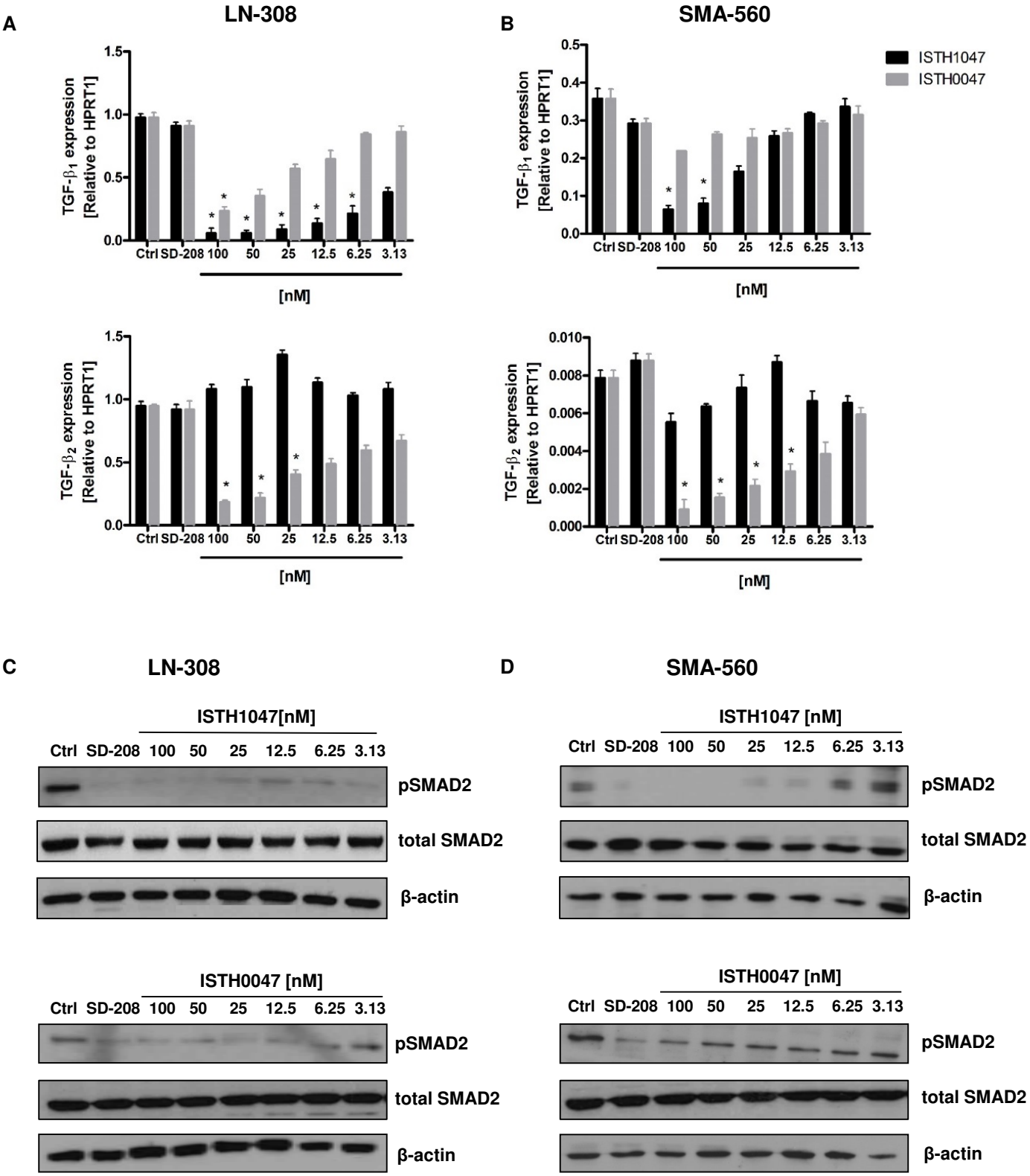

Supplementary Figure 4

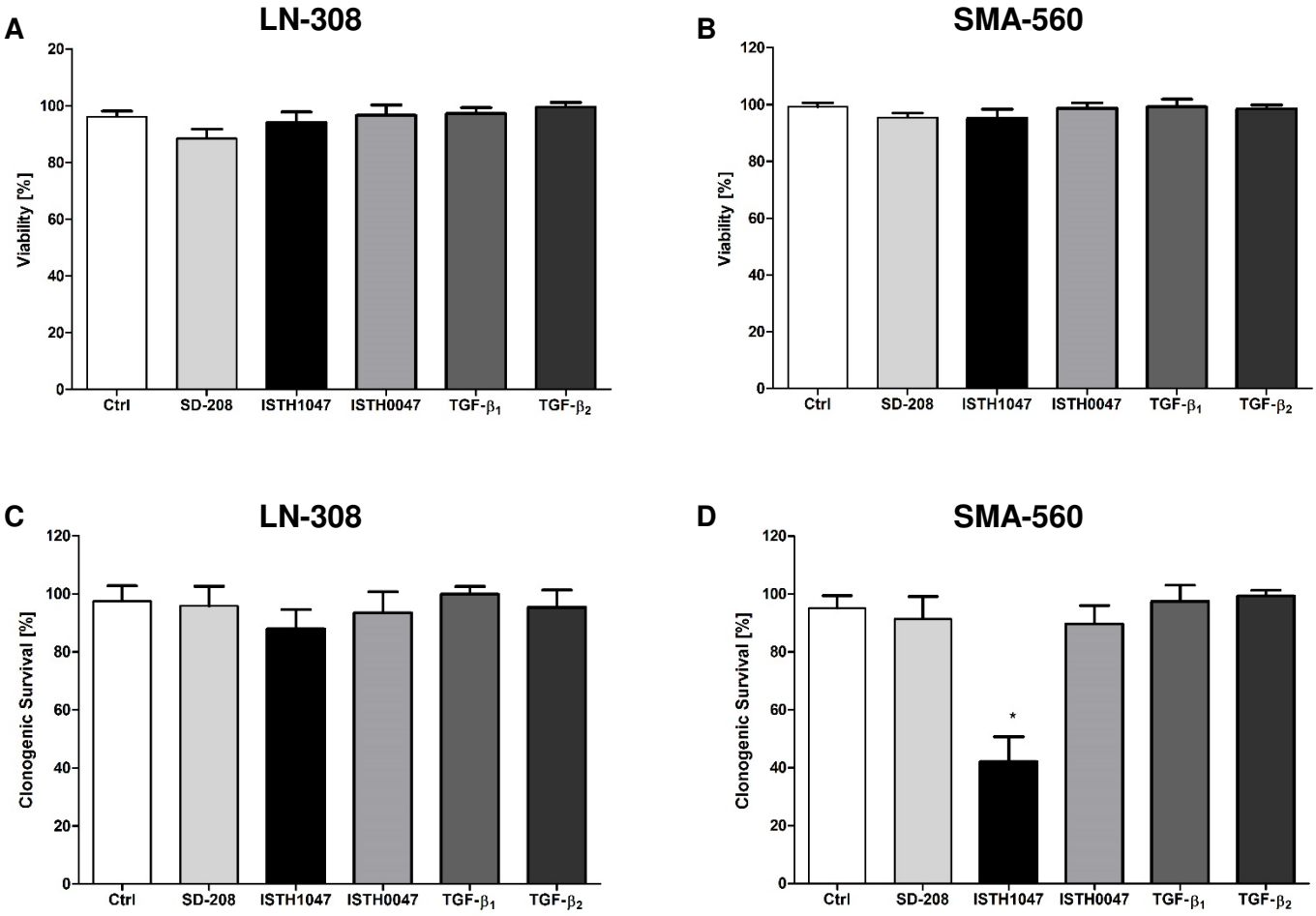

Supplementary Figure 5

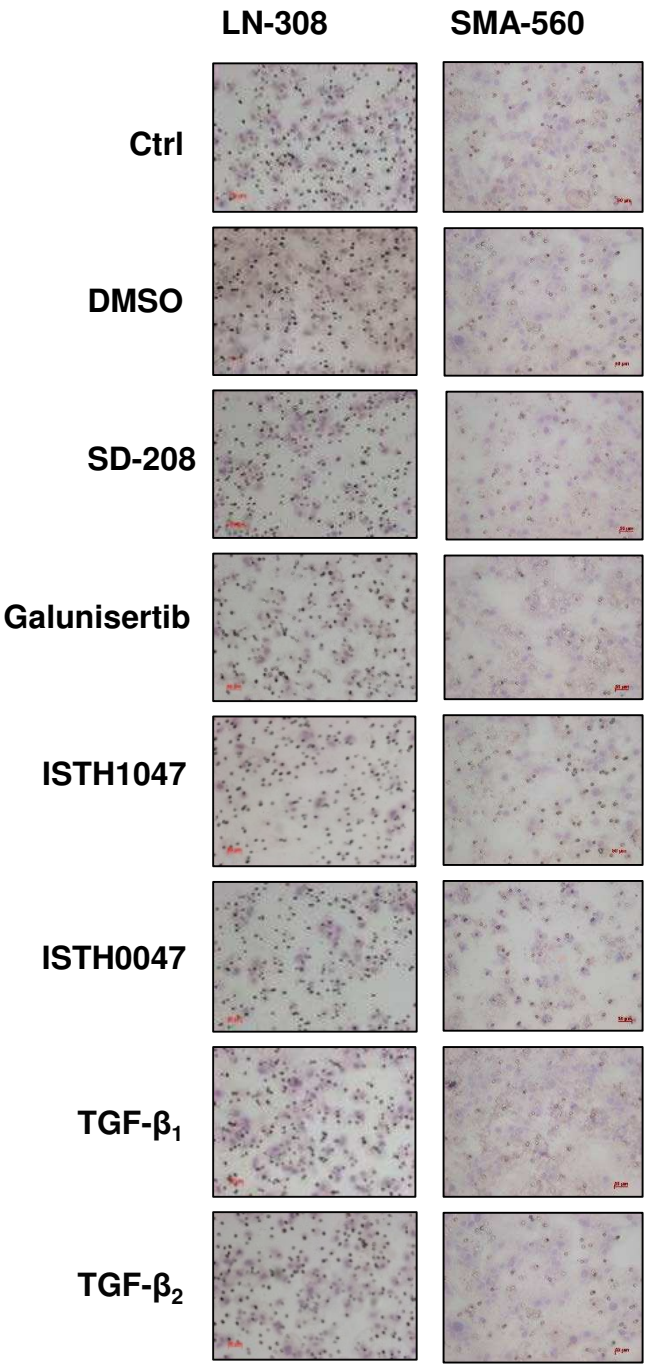

Supplementary Figure 6

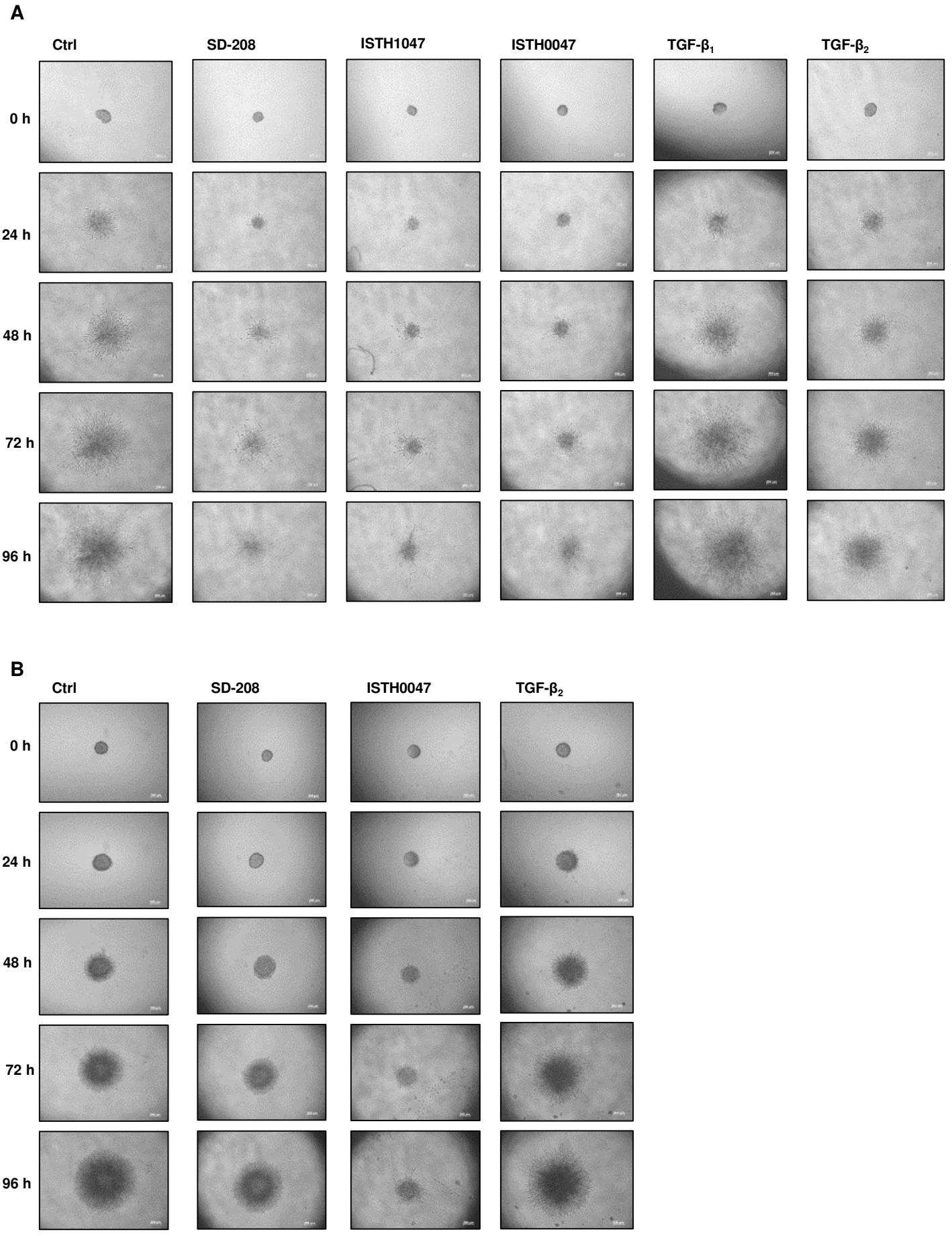

Supplementary Figure 7

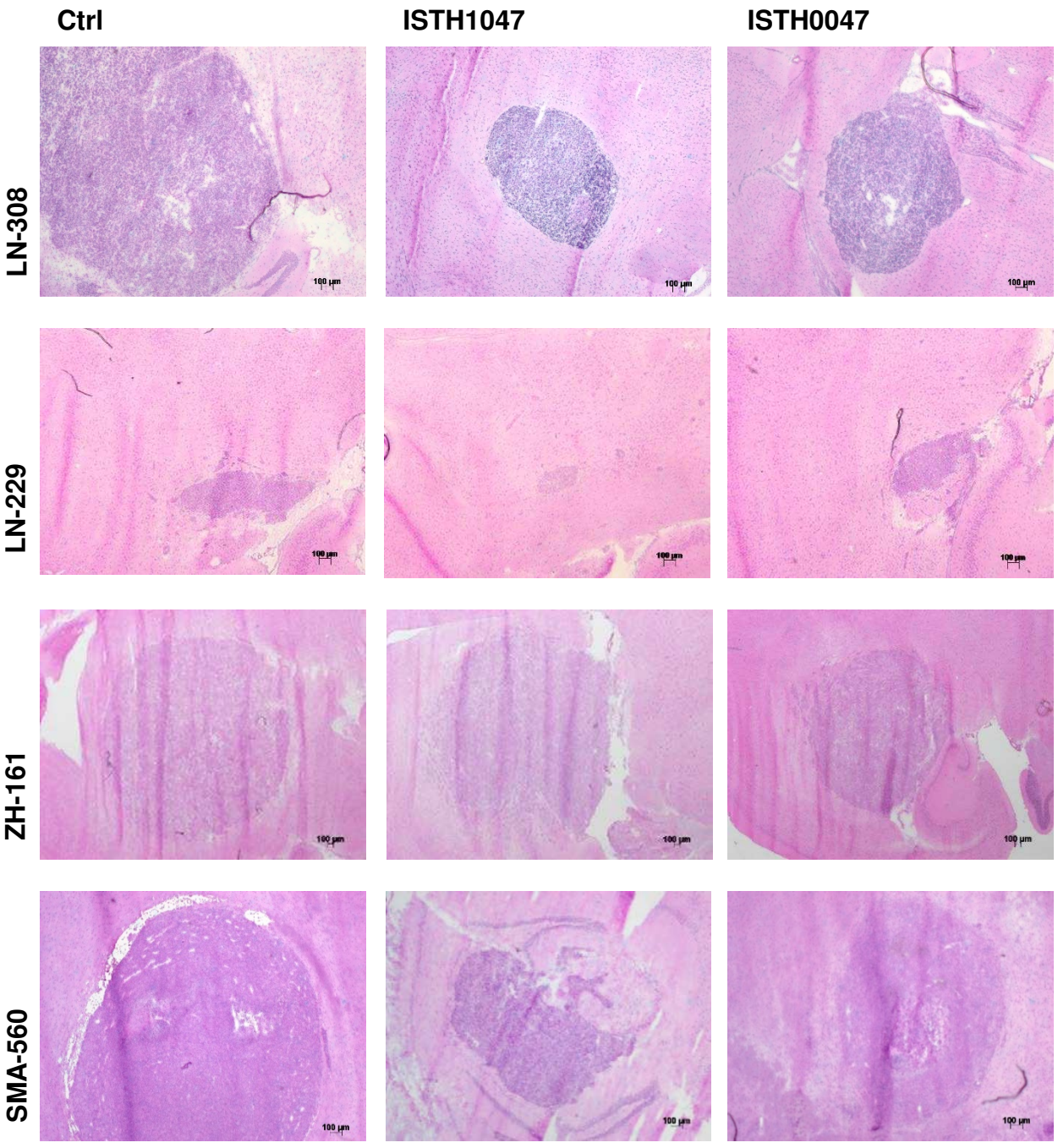

Supplementary Figure 8

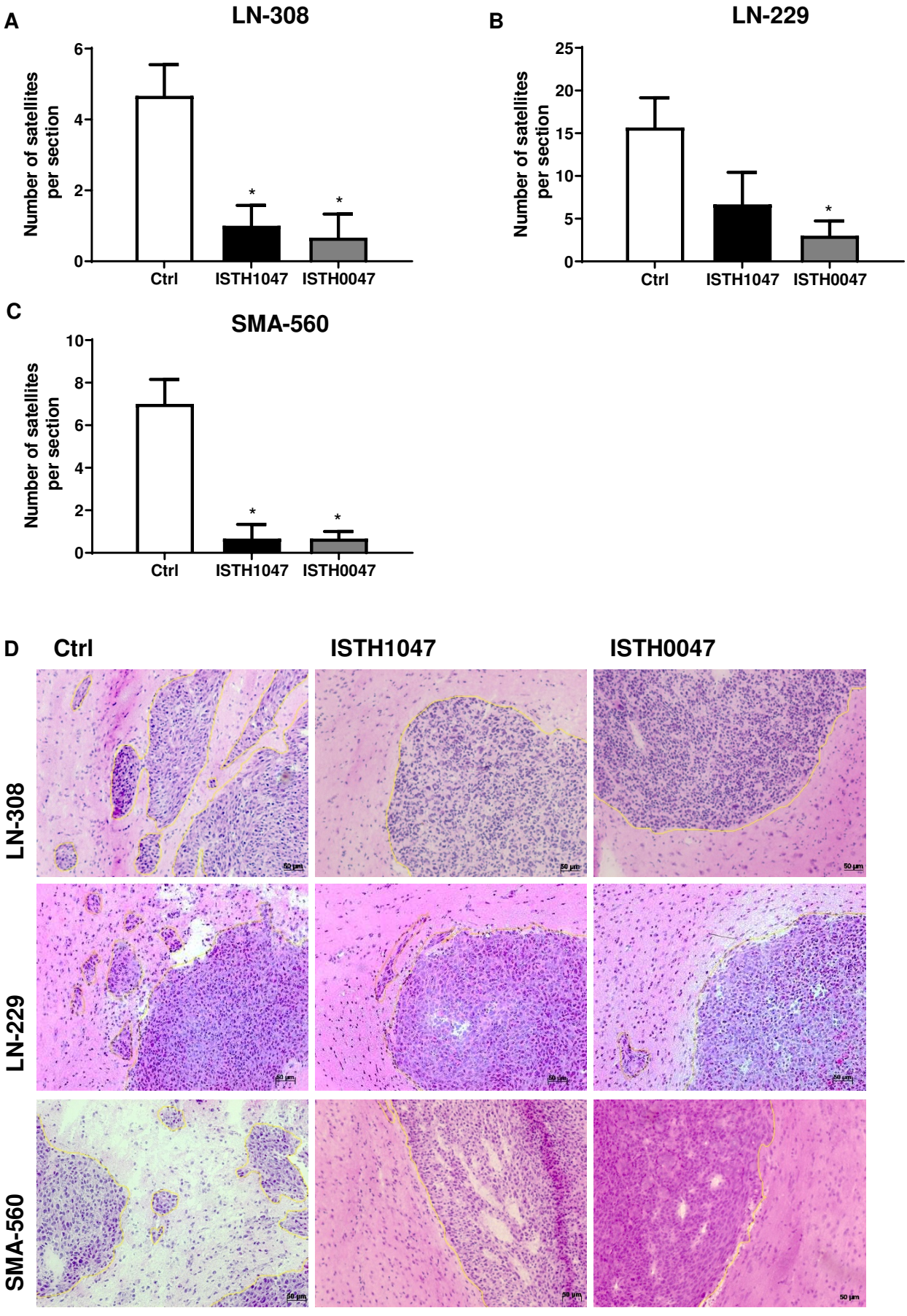

Supplementary Figure 9

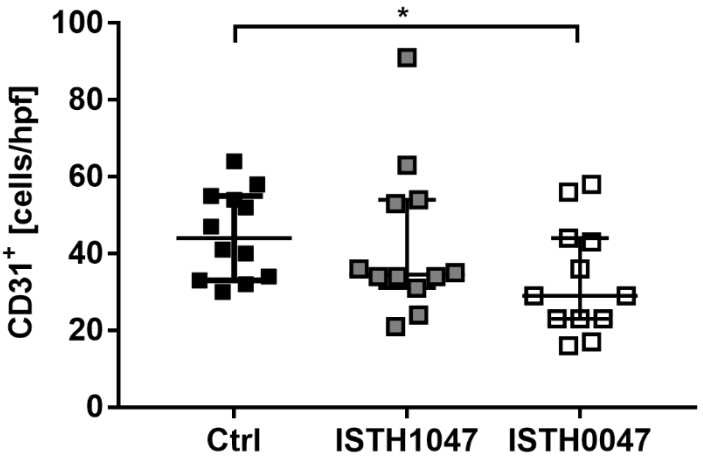

Supplementary Figure 10